Sudan University of Science and Technology

College of Engineering

Electronics Engineering Department

Performance Evaluation of Channel Model for Visible Light Communication

A Research Submitted in Partial fulfillment for the Requirements of the Degree of B.Sc. (Honors) in Electronics Engineering (Communications)

Prepared By:

1. Malaz Abubaker Abdalaziz
2. Sugod Abdallah Ahmed
3. Noon Wahba Hasbo
4. Nehad Eisa Ahmed

Supervised By:

Dr. Ibrahim Elkhider

March 2022

الأية

قال تعالى:

﴿اللَّهُ نورُ السَّماواتِ وَالأَرضِ مَثَلُ نورِهِ كَمِشكاةٍ فيها مِصباحٌ المِصباحُ في زُجاجَةٍ الزُّجاجَةُ كَأَنَّها كَوكَبٌ دُرِّيٌّ يوقَدُ مِن شَجَرَةٍ مُبارَكَةٍ زَيتونَةٍ لا شَرقِيَّةٍ وَلا غَربِيَّةٍ يَكادُ زَيتُها يُضيءُ وَلَو لَم تَمسَسهُ نارٌ نورٌ عَلى نورٍ يَهدِي اللَّهُ لِنورِهِ مَن يَشاءُ وَيَضرِبُ اللَّهُ الأَمثالَ لِلنّاسِ وَاللَّهُ بِكُلِّ شَيءٍ عَليمٌ﴾

[النور: ٣٥]

DEDICATION

This thesis is dedicated to our respective teacher **Dr. Imad Bashir** and our colleagues **Ibrahim** and **Marwa** who left us early.

PDF-XChange Editor
Click to BUY NOW!
www.tracker-software.com

ACKNOWLEDGMENT

First of all we thank the almighty Allah for giving us the strength, passion and ambience to successfully accomplish this thesis at time.

We are very thankful to our supervisor **Dr. Ibrahim Khidir** for his continuous guidance and scientific insight during this thesis.

Many thanks to Dr. **Mayada Aabdelgadir** for giving us many useful information.

We would like to thank our parents for their encouraged, and support in every field of life especially education.

ABSTRACT

Visible light communication (VLC) is an upcoming technique which can be used for data communication which uses visible light. This thesis, begin with a review of the basic (VLC) communication system mainly focus on the indoor and outdoor channel models, we designed a realistic indoor environment with multiple transmitters and receivers to distribute the LEDs on the channel, and the influence of various factors on the channel abroad. A comprehensive mathematical model is derived and simulated to investigate the performance of the proposed system considering the effect of different parameters such as received signal strength (RSS), Signal to Noise Ratio (SNR), distance between transmitter and receiver, and propagation delay in indoor (VLC), and Signal to Noise Ratio (SNR) with Bite Error Rate (BER) under different losses for outdoor (VLC) system. We reported a simulation program for indoor and outdoor visible light communication channel model based on MATLAB. Result showed that received signal strength and delay root mean square was better at small angle, and SNR was better at large angle, while minimum (BER) result with effect of smoke/fog was better than another effect of different losses outdoor VLC system.

المستخلص

الإتصالات الضوئية المرئية هي تقنية قادمة والتي يمكن استخدامها لإتصالات البيانات التي تستخدم الضوء المرئي . تبدأ الأطروحة بمراجعة نظام الاتصال الضوئي وتركز بشكل أساسي على نماذج القنوات الضوئية في الداخل والخارج .صممنا بيئة داخلية واقعية بأجهزة إرسال واستقبال متعددة لتوزيع دايود الباعث الضوئي على القناة, وتأثير الضوضاء المختلفة على القناة في الخارج. .تم اشتقاق نموذج رياضي شامل ومحاكاته للتحقيق في أداء النظام المقترح مع مراعاة التأثير على العوامل المختلفة مثل قوة الإشارة المستقبلة ونسبة الإشارة إلى الضوضاء والمسافة بين المرسل والمستقبل وتأخير الإنتشار في الاماكن المغلقة, ونسبة الإشارة الى الضوضاء تحت تأثير الضباب والدخان لنظام الاتصال الخارجي. أبلغنا عن برنامج محاكاة لنموذج قناة اتصال الضوء المرئي الداخلي والخارجي استنادًا إلى برنامج الماتلاب. والنتيجة توضح أن قوة الاشارة المستقبلة وتاخير الانتشار كانتا افضل عند اقل زاوية,بينما نحصل علي معدل خطأ للبتات أقل مع تأثير الدخان والضباب بالمقارنه مع الثأثيرات الاخرى .

TABLE OF CONTENTS

CONTENTS **PAG**

LIST OF FIGURES

LIST OF TABLES

LIST OF SYMBOLS

$y(t)$	Received signal
$x(t)$	Transmitted signal
$h(t)$	Channel impulse response
$n(t)$	Total noise
M_t	Transmitting LEDs
M_r	Receiving PDs
z	Received signal vector
H	MIMO channel
m	Noise vector
h_{jk_d}	Desired channel path
h_{jk_i}	Interference channel path
σ_j	Received noise
σ_{th_i}	Thermal noise
σ_{sh_i}	Shot noise
γ	Responsivity
d	LOS path
φ	Semi angle
P_{tr}	Average transmission optical power
A_{eff}	Affective collection area of the detector
$g(\psi)$	Optical gain of an ideal non-imaging concentrator
H_{los}	Direct current DC gain

P_a	Ambient light power detected by receiver
P_{bg}	Background irradiance per unit bandwidth
Y	Attenuation
S	Snow precipitation intensity
RI	Received Information
T_d	Transmission rate
V_s	Vehicle speed
A	Signal attenuation due to foggy weather
K	Optical attenuation coefficient
M_s	Smoke density
V_i	Visibility
P_r	Optical Power Distribution of LOS Link
Ψ	Angle of incidence
$T_s(\Psi)$	Filter transmission
$g(\Psi)$	Gain and FOV
m_i	Optimum Lambertian
B	Bandwidth of the electrical filter
K	Boltzmann's constant
IB	Photocurrent
T	FET channel noise factor
g_m	FET transconductance and noise-bandwidth factors
μ	Mean excess delay
D_{rms}	RMS delay spread
T_s	Symbol duration

ε	Extinction ratio
P_n	Noise power output
V_1	Received electrical signal corresponding to bit 1
V_0	Received electrical signal corresponding to bit 0
σ_1	Standard deviation value of received electrical signal to bits
σ_0	Standard deviation value of received electrical signal to bits
G	Transimpendace (TIA) gain
η	Rsponsivity
R_{load}	Load impedance
P_{sig}	Electrical signal power
P_{det}	Detector noise power
q	Electron charge
I	Current due to the noise
P_{bg}	Illumination power
P_n	Noise power at the output of TIA
P_{noise}	Total noise power
F_s	Sampling frequency
λ	Laser wavelength
L	Link distance
T_r	Full-angle angular field-of-view
P_{Tx}	Total power of the beam
$W_h(z)$	Beam radius along horizontal
(Z)	Vertical directions
w_{oh}	Beam radii at transmitter (horizontal)

PDF-XChange Editor Click to BUY NOW! www.tracker-software.com

w_{ov}	Beam radii at transmitter (vertical)
θ_{oh}	Beam divergence at transmitter (horizontal)
θ_{ov}	Beam divergence at transmitter (vertical)

LIST OF ABBREVIATIONS

AA	Aperture Averaging
AT	Atmospheric Turbulence
BER	Bite Error Rate
CP	Cyclic Prefix
DRMS	Delay Root Mean Square
FOV	Field Of View
IFFT	Inverse Fast Fourier Transform
I-L-PPM	Inverse L- Pulse Position Modulation
ISI	Inter- Symbol Interference
IM/DD	Intensity Modulation & Direct Detection
LEDs	Light Emitting Diode
LOS	Line Of Sight
MIMO	Multiple-Input-Multiple-Output
OFDM	Orthogonal Frequency Multiplexing
OOK	On-off keying
PD	Photo Detector
VLC	Visible Light Communication
VVLCs	Vehicular Visible Light Communication
RF	Radio Frequency
RFC	Radio Frequency Communications
RX	Receiver devices

PDF-XChange Editor Click to BUY NOW! www.tracker-software.com

RSS	Received Signal Strength
SNR	Signal to Noise Ratio
TX	Transmitter devices
QAM	Quadrature Amplitude Modulation

CHAPTER ONE

INTRODUCTION

1.1 Preface

In this thesis, we address channel modeling for visible light communication mainly focusing on indoor and outdoor systems. We introduce different sources of impairment in VLC systems arising from beam propagation or transmitter (TX) receiver (RX) devices. This technology has been considered as one of the most promising communication technologies for future wireless networks. VLCs are a viable candidate for short-range indoor applications with very high data rates. In terms of outdoor applications, Vehicular VLCs (VVLCs) play an important role in vehicular ad hoc networks and intelligent transportation Systems(ITS) [1].

1.2 Problem Statement

Indoor visible light communication suffer from interference from ambient light source and effect of different angles for parameters, while the key outdoor challenges are the weather variabilities, smoke particles, pointing error channel, and turbulence channel.

1.3 Proposed solution

To evaluate the system performance in channel modeling for both indoor and outdoor visible light communication.

PDF-XChange Editor Click to BUY NOW! www.tracker-software.com

1.4 Thesis Objective

The Objectives of This Thesis are

- To study and analyze visible light Communications.
- To study the indoor and outdoor channel models.
- To simulate and evaluate the channel models for visible light communication.

1.5 Methodology

The methodology which used to present the indoor and outdoor channel models for visible light communication is MATLAB.

1.6 Thesis Outline

The rest of the thesis include the following.

Chapter One: It is an introduction of the research and it covers the Problem Statement, proposed Solution and Objectives.

Chapter Tow: Present the background & the literature review of channel models for visible light communication.

Chapter Three: Shows the methodology of the thesis.

Chapter Four: Describe the simulation and the results.

Chapter Five: Present the conclusion and recommendations for other work.

CHAPTER TWO

LITERATURE REVIEW

2.1 Introduction

Visible light is the form in which electromagnetic radiation with wave length in a particular range is interpreted by human brain. Visible light is comprised of visually perceivable electromagnetic wave. The visible spectrum covers wave length from 380 nm to 750nm [2].

Visible Light Communications (VLC): is refer to communication technology, which utilities the visible light sources as a signal transmitter, the air as transmission medium, and appropriate photodiode as a signal receiving component. In the most recent, Couple of years, worldwide research in visible light communication (VLC) utilizing LEDs for both light and information is at the pinnacle. This technology is useful mainly due to high transmission capacity and information rate, information security, no health hazards and low power utilization. The information is encoded in radiating light in different ways and a photo detector at the receiver receives and decodes the modulated signal fulfilling the criteria of the dual purposes of illumination and communication shown in figure 2.1. In the recent years, it has been demonstrated that VLC can achieve high information rates as the communication encoded in visible light has uncommon significance relative to existing modes of wireless communication. RF waves

interfere with electronic devices and can infiltrate walls effectively prompts to the deterioration of signals and this attenuation in propagation limits information rates of proposed clients, however, visible light does not interfere with electronic devices. VLC can give required coverage, visible light cannot infiltrate walls, so it has an inalienable connection security. Visible light communication operating in the visible light range, which incorporates hundreds of terahertz of license free bandwidth shown in figure 2.2 [3].

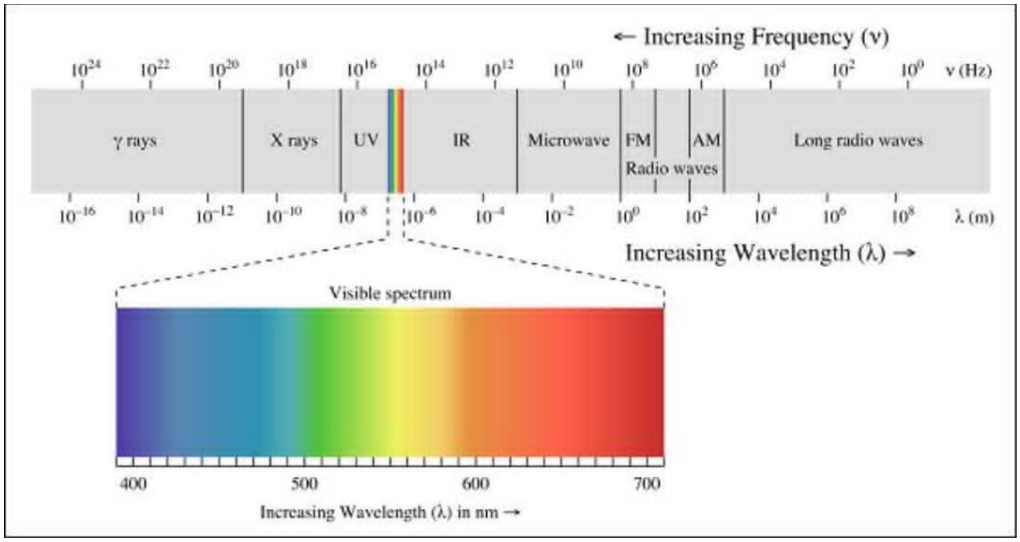

Figure 2.1 Electromagnetic Spectrum.

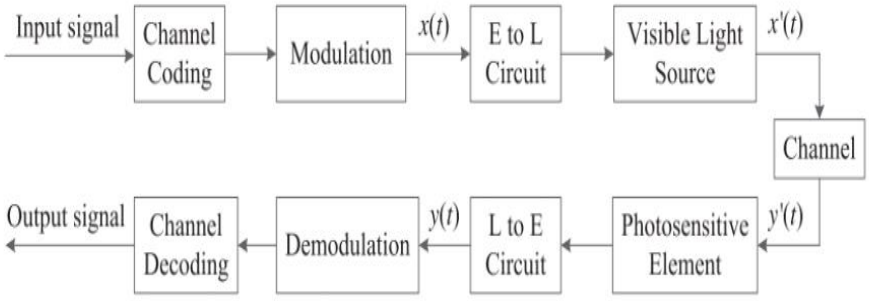

Figure 2.2 A block diagram of a typical system

2.2 Related Work

On general, there are two different types of VLC links. One is point-to-point link, and the other is diffusing link. In the point-to-point links, transceivers communicate with each other through a bunch of narrow beams, and it requires that no obstacles exist between the transceivers, and the beams should be pointed to the right directions.

The aforementioned link setup is beneficial to reduce interferences to the receiver from ambient stray light, lower signal attenuation, to achieve high data rate transmission. However, the point-to-point channels require strict LOS transmission, which is very sensitive to blocking and shadow effects. This type of VLC links has its certain advantages in terms of low cost of link setup. In the second type of VLC link, the signal radiates in accordance with a wide angle, similar to RF links. Thus, a diffusing link does not have radiation orientation and shading issues that exist in point-to-point links, and a receiver in such a link can have small mobility. At the same time, the VLC in diffusing links may suffer a loss in signal data rate and introduce multipath-induced signal distortion, which has a significant impact on the upper bound of overall channel capacity. It should also be noted that this type of links does not have diffuse multipath fading problems that are common in traditional RF wireless technologies.

The basic channel model is given as:

$$y(t) = x(t) * h(t) + n(t) \quad (2.1)$$

Where y(t) is the received signal, x(t) represents the transmitted signal, h(t) expresses the impulse response of the channel, and n(t)

PDF-XChange Editor Click to BUY NOW! www.tracker-software.com

denotes total noise including ambient noise, shot noise, and thermal noise 40.

Selection of appropriate sources depends largely on the specific applications of VLC systems. Although a white light source can be made by mixing red, green, and blue lights, the vast majority of LED lighting sources still use a blue LED with yellow phosphor coated outside. In general, a LED will scatter its light energy in all directions, rather than generate a directional beam, which is related to its own aperture design the core element of a receiver is a photo detector (PD).

This component converts the received optical signals into electrical signals, that is, the optical power into electrical current. It is known that the main parameters associated with the receiver include physical area of photodiode, the receiver's field of view (FOV), responsiveness of a detector, and so on.

Generally speaking, the receiver will utilize the assembly technique to suppress stray light noise, while allowing the optimal detection of the desirable optical signals. In addition, the receiver often comprises a light filter, an optical concentrator, an optical lens, and an amplifier connected to its rear end to ensure a sufficiently high link budget, a receiver should have a large reception area. We can employ an optical concentrator to achieve this.

An optical concentrator can significantly improve the effective signal receiving area, provide effective noise-free gain, increase the reception gain of a receiver, and avoid using a larger surface area of PD. This design is also important to achieve an optimization for power budget and can improve the transmission distance between transceivers [4].

2.2.1 Channel modeling in indoor VLCs system

In this study Visible Light Communication (VLC) is developing as a promising technique for delivering global wireless connection. This VLC is used in 5th generation and beyond wireless communication systems, specifically in indoor applications. VLC communication is secure and it is considered as a green alternative to the conventional Radio Frequency Communications (RFC).

RF-based communication causes spectrum shortage with the increasing demand for higher data rate, but the VLC has an unregulated and license-free Radio Frequency spectrum which helps to satisfy higher data rate. In VLC, the Intensity Modulation with Direct Detection (IM/DD) is used to maintain the transmitted signal as positive and real. The characteristics of VLC are IM/DD, large bandwidth and unlicensed spectrum, etc. Moreover, the main feature of the VLC that is unique from remaining optical wireless communication systems, e.g., infrared communication is that it has the capacity to deliver the illumination and communication at the same time.

The VLC technology uses the light emitting diodes (LEDs) in transmitters due to the characteristics of low cost illumination and higher bandwidth as well as the photo detectors (PDs) used in receivers. The additional characteristics of LEDs are higher lifetime, mercury-free, low power consumption and high brightness. However, system faces many challenges such as LED non-linearity, shadowing and blocking, limited mobility and Inter- Symbol Interference (ISI) due to multipath. In order

to overcome the aforementioned problems, the Multiple-Input-Multiple-Output (MIMO) and orthogonal frequency multiplexing (OFDM) are utilized for enhancing the ability of the VLC systems. The incorporation of MIMO improves the performances of VLC, especially in high range data transmission. The problems faced by the MIMO VLC system are given as follows: Generally, the MIMO VLC channel exists in static Line of Sight (LOS) conditions. The correlations due to the static LOS are associated to the LED array parameters and PDs array. The transmission performance is highly affected due to the strong correlation in the channel matrix. An effective precoding technique is to be developed for avoiding the interference and achieve user fairness.

The major contributions of this research we study are stated as follows:

•A 4×4 indoor MIMO-VLC system is developed to improve the data rate and reliability in data transmission. Here, 4×4 is defined as the installation of 4 LEDs in the transmitter side and 4 PDs in the receiver side.

• Block Bi-Diagonalization (BBD)-based precoding is presented in this communication system to remove the inferences caused due to the thermal noise, shot noise and phase noise. This is because these noise constraints affect the signal, which is transmitted through the MIMO-VLC system. Additionally, the BBD-based precoding used in this VLC system has less computation complexity.

• Quadrature Amplitude Modulation (QAM)-based modulation also improves the transmission of the MIMO-VLC transmitter. The Bit Error Rate (BER) and throughput of the proposed system are analyzed for three different scenarios under noise constraints.

In this proposed system, a BBD-based precoding is utilized to improve the BER performances in the indoor MIMO-VLC system. The precoding utilized in the proposed system leads to the reduction of the interferences occurring in the communications. Additionally, the QAM is executed during data transmission which has the efficient usage of bandwidth. The main elements present in the proposed system are QAM modulation, LED as transmitter, PD as receiver and QAM demodulation.

The block diagram of the proposed indoor MIMO-VLC system is in Figure 2.3.

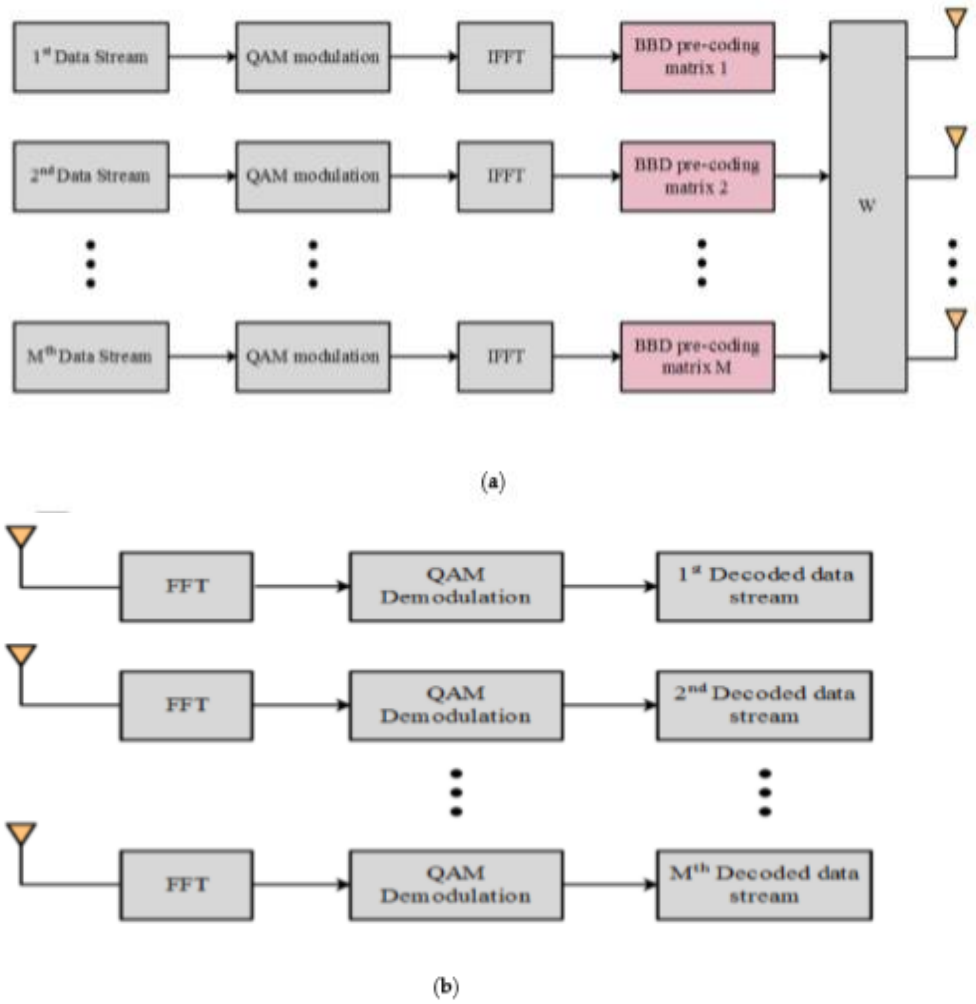

Figure 2.3 Proposed Indoor MIMO-VLC system. (a) Transmitter. (b) Receiver

System Model in the MIMO-VLC system is generally comprised of M_t transmitting LEDs and M_r receiving PDs for communication. The amount of transmitting LED and receiving PDs are the same during the communication (i.e., M_t=M_r=M). Therefore, the Mt independent data streams are transmitted simultaneously to the respective PDs. In the transmitter side, the time domain signal is acquired by using the Inverse Fast Fourier Transform (IFFT), parallel to serial conversion, and Cyclic Prefix (CP) insertion. The transmitted signals are mapped by using the QAM with the modulation order 64.

Subsequently, the BBD precoding matrix is added to transmitter data as well as the digital to analog converter used in the transmitter to convert the digital signals in to analog signals.

Similarly, the analog to digital converter is used for converting the analog signals into digital signals. In this MIMO-VLC system, the transmitted data is recovered through the removal of CP, serial to parallel conversion, Fast Fourier Transform (FFT) and QAM demodulation. The received signal at the PD is specified in Equation (2.2).

$$z = Hy + DC + m \tag{2.2}$$

Where, the received and input signal vectors through the indoor MIMO-VLC communication system are z and y, respectively. The DC bias matrix is represented as DC which is added in the transmitted signal to keep the signal as positive. The noise vector is represented as m and the MIMO channel is represented as the square matrix H. The square matrix is represented in the following Equation (2.3).

$$H = \begin{bmatrix} h_{11d} & h_{12j} & \dots h_{1Mj} \\ h_{21j} & h_{22d} & \dots h_{2Mj} \\ & \vdots & \vdots \\ h_{M1j} & h_{M2j} & \dots h_{MMj} \end{bmatrix} \quad (2.3)$$

Where, the desired and interference channel paths are represented as h_{jk_d} and h_{jk_i}, respectively.

Equation (2.4) depicts the receiver noise that occurred while transmitting the data through the MIMO-VLC transmitter.

$$\sigma_j^2 = \sigma_{sh_i}^2 + \sigma_{th_i}^2 \quad (2.4)$$

By considering the aforesaid measures, a parallel signal-to-interference-plus-noise ratio (SINR) in j_{th} PD is expressed as in Equation (2.5).

$$SNR_j = \frac{(\gamma P h_{jj})^2}{\left(\gamma^2 P^2 \sum_{K=1,K\neq j}^{M} h_{jk}^2\right) + \sigma_j^2} \quad (2.5)$$

The experimental results and comparative analysis of the proposed system are described in this section. The implementation and simulation of the indoor MIMO-VLC system using precoding is carried out in MATLAB R2018a with 4GB RAM and an i3 processor.

The main objective of the indoor MIMO-VLC communication using BBD precoding is to mitigate the interferences in the data transmission. The specifications used for the LED transmitter and PD receiver are specified in Table 1.

In this proposed system, the LEDs are initialized with the power of 10 mW. Moreover, the semi angle of transmitter and FOV of PD

receiver are fixed as 15◦. Here, the 4×4 indoor MIMO-VLC model is considered to analyze the communication performances [5].

Table 1 Indoor VLC parameters

Parameters of LED Transmitter	
Amount of LEDs per luminary	60×60
LED transmitter power	10 mW
Semi angle of transmitter	15◦
Parameters of PD Receiver	
FOV of receiver	15◦
PD area	1.0 cm2
PD responsivity	1 A/W
PD lens' refractive index	1.5
Gain of optical filter	1.0
Background current	100 µA
Bandwidth factor of noise	0.562

In another study they consider an empty room size of 5m×5m×3m where four LED luminaires are located on the ceiling and the detector is located at the corner of the floor as illustrated in figure2.4 (a). An LED luminaire consists of 100 LED chips and each chip radiates 0.45W with a full angle of half power of 120°. The FOV and area of the detector are 85° and 1cm2, respectively.

They use Cree X lamp MC-E White LED figure2.4 (b) which has nearly ideal lambertian pattern. They elaborated on the site-specific channel modelling approach based on non-sequential ray tracing. Using

this approach, they obtained sample CIRs for a typical indoor environment with multiple light sources. It was observed that multiple LOS components might be present in the CIR due to the availability of multiple sources. Based on the distances between light sources and receiver locations, some of these LOS components are not resolvable.They further investigated the effect of higher order reflections, which highly depends on the type of reflections. Their results demonstrated that while higher order reflections larger than four is negligible for a typical room size assuming diffuse reflections, up to eight reflections should be considered for a more precise characterization under the assumption of mostly specular reflections [6].

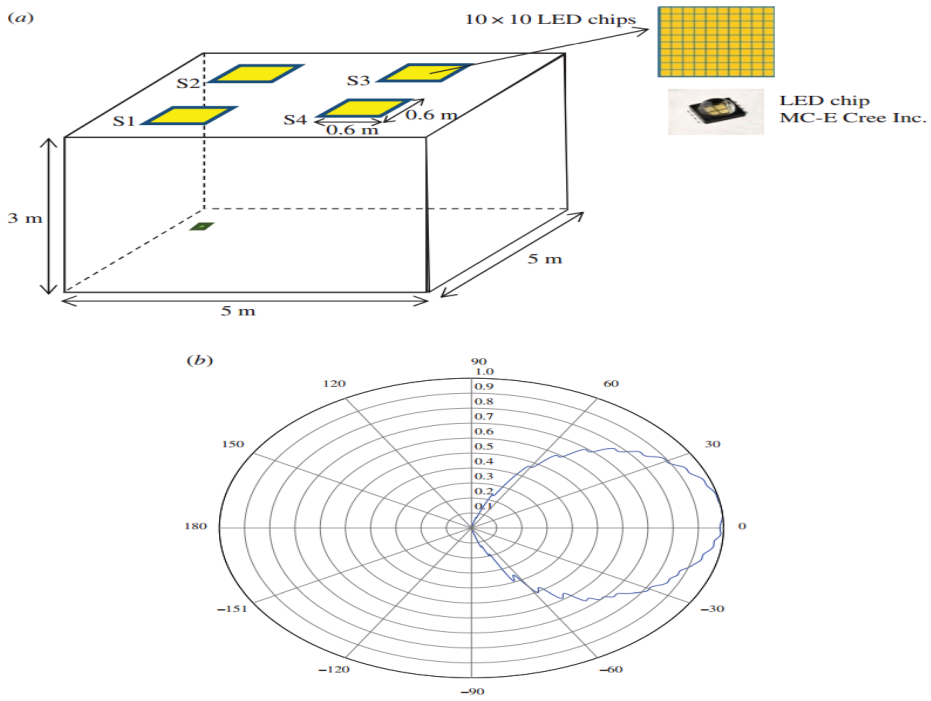

Figure2.4 (a) Three-dimensional environment and (b) emission pattern of source.

In this study an indoor with a single transmitter and a single receiver is considered. The Lambertian emission-based channel model and the on-off keying (OOK) are employed. In the system, the noises

include two parts: input-dependent noise and input independent noise. In the presence of two kinds of noises, the BER of the system is analyzed.

As a special case, the BER with only the input-independent noise is also shown. By minimizing the BER, an optimization problem is formulated to improve the system performance.

Then, the optimization problem is solved by using the principle of the convex optimization. After solving the problem, the optimal tilting angle of the receiver is obtained.

The derived theoretical results of BER are all confirmed by using the Monte-Carlo simulations. The optimization problem was to minimize the BER by using the principle of convex optimization, the optimization problem was effectively solved the implementation of the optimal tilting angle was discussed the optimal tilting angle is a function of the positions of the LED and the PD.

The position of the LED(i.e.,[u ,v ,w]) is fixed ,but the position of the PD(i.e.,[a ,b ,c]) is variable according to the optimal tilting angle, the receiver can realize the angle tilting by employing an electrical machinery the electrical machinery first makes the tilting angle to be zero and then increases the tilting angle until the optical tilting angle is achieved figure2.5.

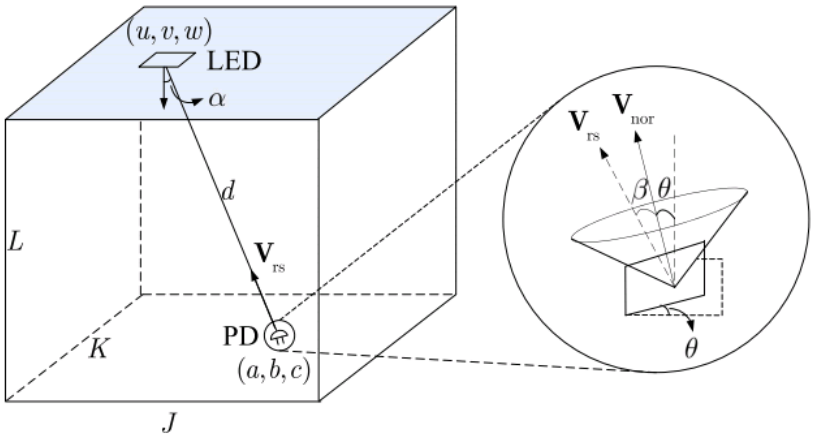

Figure2.5 A classic point-to-point indoor VLC system

For the VLC system with input-dependent noise the optimal detection threshold is obtained also the oretical expression of the BER is derived which is quite accurate to evaluate the system performance the system performance is strongly affected by the input-dependent noise .For small h or p the BER decreases with the increase of ς.

However for large h or P the trend of the BER curve changes Moreover, the larger the value of the channel gain is the better the BER performance becomes When the transceiver distance is large the BER performance can be dramatically enhanced by tilting the receiver plane in practice, the suggested tilting angle of the receiver place [7].

2.2.2 Channel Modeling in Outdoor VLC System

A comprehensive study of outdoor visible light communication (VLC) under snow and rain effects has been conducted in this study, this study analyzes the expected rain attenuation of Marshal, Carbonneau and Japan models at different precipitation levels. Snow attenuation is measured in wet and dry situations at various precipitation levels as well. Therefore, a full comparison is carried out for different attenuation effects on certain outdoor VLC design characteristics such as the

maximum signal-to-noise ratio (SNR), optical power received, Bit error rate (BER), and maximum coverage area. VLC with various modulation techniques is considered. The ON–OFF Keying (OOK), L-Pulse Position Modulation (L-PPM), Inverse L-Pulse Position Modulation (I-L-PPM), and Subcarrier Binary phase shift keying (SC-BPSK) are investigated.

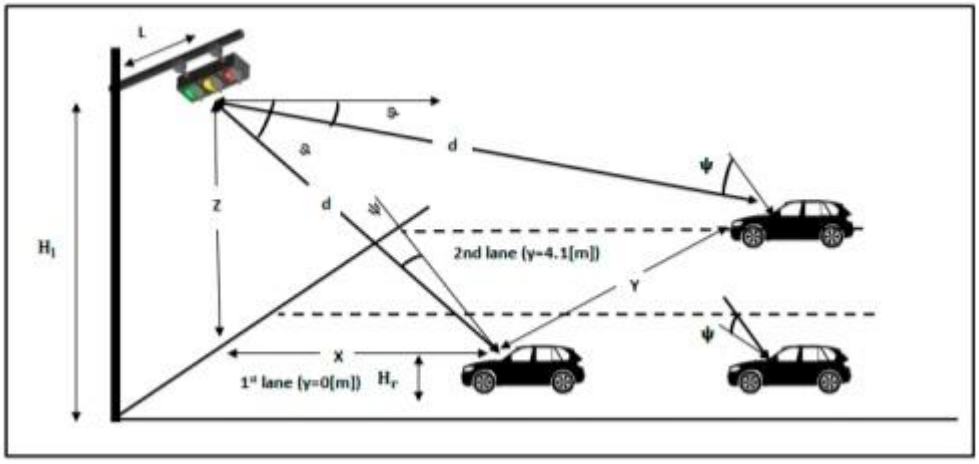

Figure2.6 Two-lane traffic light system model

The LOS path, d, between the transmitter and the receiver is given as

$$d = \sqrt{x^2 y^2 z^2} \tag{2.6}$$

Both angels φ *and* ψ are calculated respectively ,from figure 1 as

$$\varphi = cos^{-1}\frac{x}{y} \tag{2.7}$$

The emission power from LED transmitters P_{tr} can be calculate as

$$\Psi = cos^{-1}\frac{sin\theta + tan^{-1}\frac{z}{x}\sqrt{x^2+z^2}}{d} \tag{2.8}$$

$$p_{tr=}\left\lfloor\frac{m+1}{2\pi}\right\rfloor \tag{2.9}$$

Where $p_{tr}$is the average transmission optical power, and the order of Lambertian emission m is related to a half power semi-angle $\varphi_{1/2}$ by

$$m = \frac{\ln(2)}{\ln(cos\varphi_{1/2})} \tag{2.10}$$

The effective collection area of the detector A_{eff}, is given by

$$A_{eff}(\Psi) = \begin{cases} AT(\psi)g(\Psi)\cos(\psi), & 0 \le \psi \le \Psi c \\ 0 & , \quad \psi > \Psi c \end{cases} \tag{2.11}$$

The optical gain of an ideal non-imaging concentrator having an internal refractive index n

$$g(\psi) = \begin{cases} \frac{n^2}{\sin \Psi c^2}, & 0 \le \psi \le \Psi c \\ 0 & \psi > \Psi c \end{cases} \tag{2.12}$$

The output signal can be calculated as

$$y(t) = x(t) * h(t) + n(t) \tag{2.13}$$

The direct current DC gain H_{los}

$$\mathrm{H_{los}} = \begin{cases} \frac{(\mathrm{m+1})\mathrm{A}}{2\pi \mathrm{d}^2}\cos\varphi^{\mathrm{m}}\,\mathrm{T}(\psi)\mathrm{g}(\psi)\cos(\psi) & 0 \le \psi \le \psi \mathrm{c} \\ 0 & \psi > \Psi c \end{cases} \tag{2.14}$$

The absorption and scattering of light through the atmosphere are figured by the exponential Beers–Lambert Law

$$\tau(d) = e^{-\gamma(\lambda)d}$$
(2.15)

The desired power in the APD receiver can be obtained as

$$Prx - los = P_{tr}(\varphi).H_{los}(0)$$
(2.16)

The received signal is given by

$$Rx = Prx - los(t) + noise$$
(2.17)

The total noise variance is approximately given by approximately given by

$$\sigma^2\text{tot} \approx 2\text{q}(p_{rx} - \text{los} + p_a)\text{B} + \frac{8\pi KbT}{G}\eta A I_2 B^2 \frac{16\pi^2 kbT}{g_m}\eta^2 A^2 I_3$$
(2.18)

The ambient light power detected by receiver can be calculated as

$$P_a = P_{bg}\Delta\lambda A I_2$$ (2.19)

Where P_{bg} is the background irradiance per unit bandwidth and $\Delta\lambda$ is the filter.

Atmospheric Turbulence Analysis

The geometric optics limit can be applied to get the attenuation

$$Y = a.R^b$$ (2.20)

Table2.2 Attenuation parameters due to rain

Location/Model	A	B
Marshall and palmer	0.365	0.63

Carbonneau-France	1.076	0.67
Japan	1.580	0.63

Snow Attenuation

The attenuation, snow (dB/km), as a function of snow precipitation intensity, S (mm/h), is given by

$$\gamma snow = as^b \tag{2.21}$$

Table 2.3 Estimated values for wet and dry snow are listed

Snow Type	A	B
Wet	0.000102*λ+3.79	0.72
Dry	0.000102*λ+3.79	1.38

Modulation Schemes Analysis calculating the necessary SNR to achieve the target BER is important.

The SNR is obtained as

$$SNR = \frac{r^2 P_{rx-los}^2}{\sigma_{tot}^2} \tag{2.22}$$

The BER for the OOK scheme is actually obtained by the same equation as in the 2-PPM case which is given by

$$BER_{ook} = Q\left(\sqrt{SNR}\right) \tag{2.23}$$

Where

$$\mathrm{Q} = \frac{1}{2\pi}\int_{\mathrm{x}}^{\infty} e^{\frac{-y^2}{2}}\, dy \tag{2.24}$$

The BER performance for SC-BPSK, L-I-PPM, and L-PPM can be obtained as

$$\mathrm{BER_{sc-BpsK}} = \mathrm{Q}\left(\sqrt{\frac{\mathrm{SNR}}{2}}\right) \tag{2.25}$$

$$\mathrm{BER_{L-PPM}} = \mathrm{Q}\left(\sqrt{\mathrm{SNR}}\sqrt{\log_2 \mathrm{L}}\right) \tag{2.26}$$

$$\mathrm{BER_{1-L-ppm}} = \mathrm{Q}\left(\sqrt{\mathrm{SNR}}\sqrt{\frac{\log_2 \mathrm{L}}{\mathrm{L}-1}}\right) \tag{2.27}$$

Received Information

$$RI(bit) = \frac{T_d\left(\frac{bit}{s}\right).SA(m)}{\mathrm{v_s(km/h)}} \tag{2.28}$$

Where T_d is the transmission rate while V_s is the vehicle speed.

This implements a mathematical model to analyze the impact of very clear weather, rain, and snow attenuation on a VLC system. The effect of this attenuation has been observed through simulation of an infrastructure-to-vehicle (12V) outdoor application system, the two kinds of snow used are wet and dry, which are measured at different perception rates. Rain attenuation is measured for three different models: Marshall, France and Japan. This kind of attenuation influences light communication via light absorption or scattering and increases with the increase of communication distance. The proposed system performance is measured by its P(rx) SNR, BER, coverage area, and the amount of received information. In the case of snow, it is found that the system is more attenuated by dry snow than by wet snow. Under heavy dry snow weather, a vehicle can receive−23.08 dB_m power with 30.11 dB SNR at 18 m. For rain attenuation, the Japan model is found to be more accurate on high rainfall rates and shows a large impact on system compared with other models. At 18 m, a vehicle can receive –16.8 dB_m power with 42.44 dB SNR in heavy rain weather regarding the Japan model. Setting θ to 80◦ and the FOV to 10◦ I is more appropriate for a communication

PDF-XChange Editor
Click to BUY NOW!
www.tracker-software.com

distanceupto300m from the traffic light. The SNR for OOK, SC-BPSK, L-PPM, and I-LPPM has been determined to obtain a BER of 10^{-6}. The L-PPM can cover larger distances with lower SNR values as long as L increases under different weather conditions. On the other hand, I-LPPM can cover less distance with higher SNR values as long as L increases under different weather conditions. Comparing OOK with SC-BPSK, the last is found to cover a shorter distance with higher SNR values. The maximum achievable distance and the amount of received information depend on the type of modulation scheme used, which has been calculated. Since the amount of received information depends on the type of modulation scheme used that supports higher coverage distances, L-PPM is found to be the best scheme [8].

While another study aim to set the quantification of the weather and smoke particles' impact on a short- range optical communication. This article's novelty is the inclusion of the effects of smoke in a short-range outdoor VLC system channel model. This smoke model, which comes from the fire engineering field, states that smoke attenuation is independent of the wavelength, starting from high visibility to 5 m. The visibility represents the distance up to which an object can be distinguished against the background. The effects of fog and smoke are studied in the case of two outdoor VLC scenarios. Smoke and fog models have analogous equations to express the optical attenuation they induce, using the visibility concept, taking into account the actual light-emitting diode (LED) lamp radiation pattern, the simulator computes the power at the receiver side and the channel attenuation coefficients for a given fog or/and smoke outdoor setting. The main result drawn in this study is that the channel attenuation levels due to fog and smoke are both

in the same order of magnitude, starting from the visibility of about 1 km.

The attenuation induced by fog is higher under this threshold of 1 km, the optical power received, P_r in a line-of–sight (LOS) configuration is computed as follows.

$$pr = ptH(0)ptR(\theta,\varphi)g(\psi c)\frac{ARX}{d^2}\cos(\psi) \quad (2.29)$$

Where P_t is the power transmitted by the source and H(0) is the DC channel gain used in this context indeed in pure LOS, the channel is supposed to be flat, so H(f) = H(0).

In Equation (2.23) the channel gain can computed by

$$g(\Psi) = \frac{n^2}{(\sin\Psi)^2} \quad (2.30)$$

In a non-LOS (n Lo S) configuration

$$pr = pt\left(H(0)H^{refl}\right)$$

$$= pt9(H^0 + \sum_{i=1}^{k}(\rho iR(\varphi)g(\psi c)\frac{ARX}{d_1^2 d_2^2}\cos\psi + h^{k-1} \quad (2.31)$$

Atmospheric and Smoke Particle Theory light waves are prone to an additional attenuation by interacting with atmospheric particles found in fog, rain, and smoke.

$$\tau(L) = \frac{pr}{pt} = e^{-yL} \quad (2.32)$$

$$\gamma = \alpha_{ml} + \alpha_{al} + \beta_{ml} + \beta_{al} \quad (2.33)$$

The total attenuation from Equation (2.34) becomes the following:

$$\gamma = A + k \tag{2.34}$$

A clear sky has higher visibility than a thick fog. This parameter is used to compute the signal attenuation due to foggy weather, thanks to Kim's model:

$$A = \frac{3.91}{vi}\left(\frac{\lambda}{550}\right)^{-q} km^{-1} \tag{2.35}$$

$$q = \begin{cases} 1.6, & vi > 50km \\ 1.3, & 6km < vi < 50km \\ 0.16v + -0.34, & 1km < vi < 1km \\ v - 0.5, & 0.5km < vi < 1km \\ 0, & vi < 0.0km \end{cases} \tag{2.36}$$

Smoke Attenuation in fire engineering some laser tools are using the optical properties of smoke to compute the density of smokes produced from a given fuel. Indeed, the relationship between the optical attenuation coefficient, K, in m^{-1}, and the smoke density ,Ms, in g/m3.

$$\mathrm{I(L)} = \mathrm{I_0 e^{-kL}} \tag{2.37}$$

$$K = K_m M_s \tag{2.38}$$

$$K_m = \frac{632.8}{\lambda} 8.5 \tag{2.39}$$

Relationship between visibility and the attenuation coefficient when the object is powered and emits light (V_i) and when it is only a

reflecting sign (V_i'), respectively, V_i is the visibility computed in meters, and K is the optical attenuation coefficient found in Equation (2.40).

$$KV_i = 8 \quad (2.40)$$
$$KV_i' = 3 \quad (2.41)$$

Methodology used to develop and Assess the Python Simulation Tool Figure (2.8) shows the inputs and outputs of the simulator the input variables are the emitter and receiver characteristics, the room (number of walls) configuration and the environmental conditions.

The simulator computes the optical power received on a given receiver plane.

Radiation Patterns: Lambertian for Scenario 1 and tabulated for Scenario 2

$$R(\theta) = \frac{m+1}{2\pi}(\cos(\theta))^m \; for \theta \in [0, \pi] \quad (2.42)$$
$$m = \frac{\ln(2)}{\ln(\cos(\theta 1/2))} \quad (2.43)$$

The main conclusion drawn from the results is that the attenuation coefficient values in both scenarios are much smaller than the power margin. This means that VLC communication will always be functional outdoors, these are promising results for the deployment of outdoor VLC use cases such as VLC–IoT systems, urban Li-Fi, and geolocation. However, improvements that still need to be addressed are considering other parasitic noises at the emitter and receiver side, the presence of artificial lighting or sunlight, the real radiation pattern of the LED considered because perfect Lambertian is assumed in this work [9].

This study presents the investigation results concerning the negative effects of noise on the data signal in the case of Visible Light Communications (VLC). The motivation of this work was to offer a better understanding of the modifications of the data pulse in the presence of noise. Better understanding of the noise effect on the pulse width can help mitigate it and improve the communication performances. The paper also aims to make a comparative evaluation of two coding techniques used for outdoor VLC. The Manchester code as the code specified by the IEEE 802.15.7 standard in the case of outdoor applications using On-Off-Keying (OOK) modulation and the Miller code, as a possible alternative for Multi Input Multi Output (MIMO) applications. Simulations were performed on messages coded using the two codes for different levels of noise it seems that in the case of digital processing, the Miller code pulse is less affected by distortions caused by noise. However, in the case of the Manchester code, the higher error tolerance compensates for the pulse distortions. Regarding the Bit Error Ratio (BER), the two codes exhibit similar performances [10].

The noise influence on the VLC channel:

The VLC performances are strongly influenced by the communication channel

$$y(t) = RX(t) * h(t) + Ntotal(t) \tag{2.44}$$

The noise affecting the VLC channel (N total) contains a shot noise component and a thermal noise component, as expressed in eq (2.45)

$$Ntotal = \sqrt{N_{shot}^2 + N_{thermal}^2} \tag{2.46}$$

The results show that as the SNR decreases, the pulse widths are more and more affected by distortion, which causes decoding errors. It can be observed that due to its nature, the Miller coded signal is better filtered, but it is affected by stricter tolerances limit, which is the main cause for errors. In the case of the Manchester code, the digital filtering is less effective but it catches up due to its higher tolerance to pulse width variations. Under these circumstances, the two codes have similar BER results. Since the Manchester and the Miller code have similar performances, but as the Miller code has better channel usage, it can be considered that the Manchester code is adequate for single channel communication, the Miller code is better suited.

In this study, they investigate the performance of a vehicular visible light communications (VVLC) link with a non-collimated and incoherent light source (a light-emitting diode) as the transmitter (Tx) and two different optical receiver (Rx) types (a camera and photodiode (PD) under atmospheric turbulence (AT) conditions with aperture averaging (AA). First, we present simulation results indicating performance improvements in the signal-to-noise ratio (SNR) under AT with AA with increasing size of the optical concentrator.

System Description:

AT Parameters and Models

AT is an effect that arises from disparities in both the temperature and pressure of the atmosphere along the communications path.

n (in m−2/3) is most commonly used to describe the strength of AT which is given by :

$$C_n^2 = \left(79 * 10^{-6} \frac{p}{T^2}\right)^{2C_t^2} \quad (2.47)$$

Another important parameter, which is adopted to reflect the AT regime, is the Rytov varianceσ_R^2, which indicates the irradiance fluctuations of the optical signal resulting from AT and is given as

$$\sigma_R^2 = 1.23 C_n^2 k^{\frac{7}{6}} L_s^{\frac{11}{6}} \quad (2.48)$$

VLC System

The average SNR without and with the AT for a point Rx (i.e., with no OC) for OOK signaling are given, respectively

$$SNR(0)_0 = \frac{(p_t RH(0))^2}{\sigma_T^2(0)} \quad (2.49)$$

$$SNR(0)_{AT} = \frac{SNR_0}{\sqrt{1+\sigma_1^2(0) SNR(0)_0^2}} \quad (2.50)$$

Using an OC (i.e., aperture averaging), the average SNR with and without the AT are given as

$$SNR(0)_0 = \frac{(p_t RH(0))^2}{\sigma_T^2(D)} \quad (2.51)$$

$$SNR(0)_{AT} = \frac{SNR_0}{\sqrt{1+\sigma_1^2(D) SNR(D)_0^2}} \quad (2.52)$$

The average BER is given as

$$BER = Q\left(\sqrt{SNR}\right) \quad (2.53)$$

The results obtained showed a performance improvement in terms of the SNR under weak to moderate turbulence regimes with an increasing diameter of the receiver lens. Moreover, results also revealed that, for an increasing beam divergence angle (half power angle) the inter-link BER degradation decreased with and without turbulence.

Furthermore, we experimentally investigated the effects of aperture averaging for the VVLC link under turbulence using an LED-based vehicle's taillight. The results obtained showed that with the aperture averaging there was no significant system performance degradation under atmospheric turbulence, whereas both PSNR and SNR dropped by 0.7 and 0.1 dB for the camera and PD- Rxs, respectively, compared with the clear channel, finally we demonstrated that in VVLC systems employing incoherent non-collimated LED light sources as the Tx, the aperture averaging method proved to be very potent at mitigating weak to moderate turbulence regimes, and in fact also increased the optical power density of the received signal at the Rx [11].

CHAPTER THREE

METHODOLOGY

3.1 System model

This chapter contains two parts: firstly; Mathematical Model of Performance indoor VLC system for room area with optimal optical power distribution and signal to noise and delay spread analysis in multiple input multiple output scenario, secondly; Mathematical Model of Performance outdoor VLC system bit error rate with signal to noise ratio. MATLAB simulation tools used to apply the system proposal.

3.1.1 Indoor VLC System Model

The model is applicable for a specific room configuration and does take account of shadowing and furniture to consider the effects of people within the room, as shown in Figure 3.1.

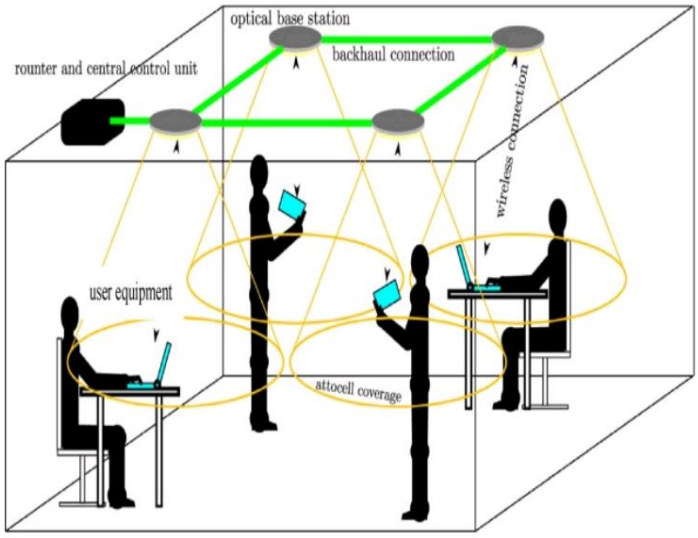

Figure 3.1 Typical room environment

3.1.1.1. Optical Power Distribution of LOS Link

$$\boldsymbol{P_r = P_t \frac{(mi+1)}{2\pi d^2} (\cos(\emptyset))^{mi} T_s(\psi) g(\psi) \cos(\psi),} \qquad 0 \leq \Psi \leq \Psi_{con} \tag{3.1}$$

.

Where: ψ is the angle of incidence with respect to the axis normal to the receiver surface, $T_s(\Psi)$ is the filter transmission, $g(\Psi)$ and Ψ_{con} are the concentrator gain and FOV, respectively and d is the distance between the VLED and a detector surface, and (m_i) is optimum Lambertian.

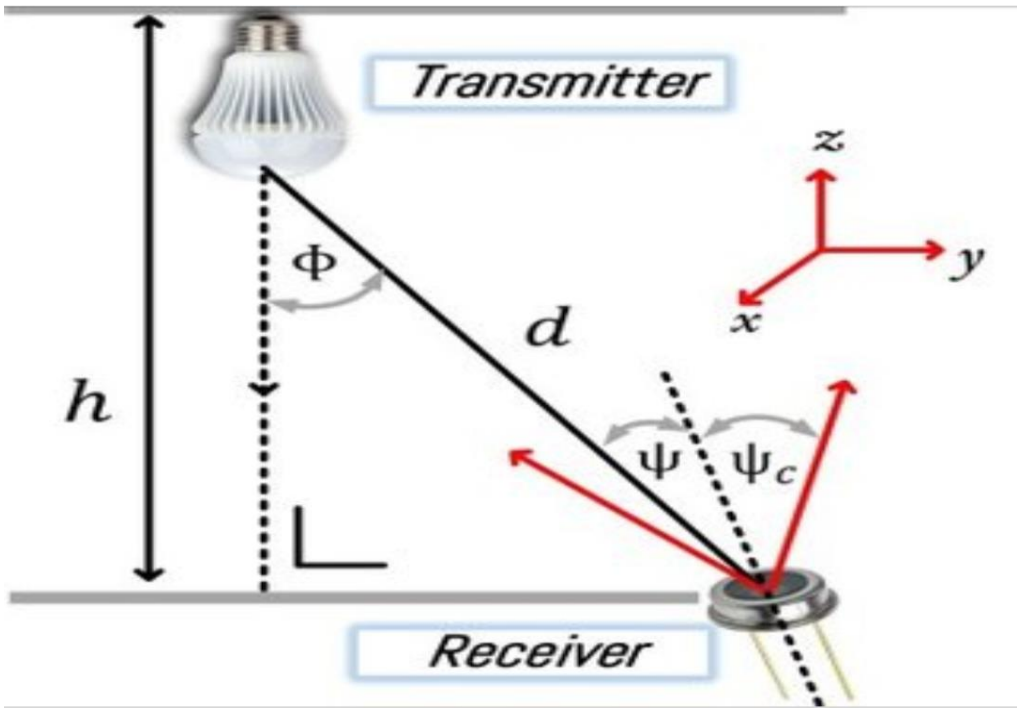

Figure 3.2 Geometry LOS propagation model

3.1.1.2 Signal to noise ratio analysis

The electrical SNR can be expressed in terms of the photo detector responsively R, received optical power and noise variance as

$$SNR = \frac{RP_t^2}{\sigma_{shot^2} + \sigma_{thermal^2}} \tag{3.2}$$

The shot and thermal noise variances are given by

$$\sigma_{shot} = 2qRP_t^2B + 2qI_BI_2B \tag{3.3}$$

$$\sigma_{thermal} = \frac{8\pi KT_K}{G_{ol}} G_{pd} AI_2B^2 + \frac{16\pi^2 KT_K T}{g_m} G_{pd}^2 AI_3B^3 \tag{3.4}$$

where the bandwidth of the electrical filter that follows the photo detector is represented by B Hz, K is the Boltzmann's constant, I_B is the photocurrent due to background radiation,T_k is absolute temperature,G_{ol} is the open-loop voltage gain, $C_{pd}$is the fixed

capacitance of photo detector per unit area, Γ is the FET channel noise factor g_m is the FET transconductanceand noise-bandwidth factorsI_2 = 0.562 and I_3= 0.0868.

3.1.1.3 Delay spread analysis

The received optical power at a point for both the direct and the first-order reflected paths is given in Equation (3.5) for multipath scenario, the total received power is given by

$$P_{rT} = \sum_{i=1}^{M} P_{d,i} + \sum_{j=1}^{N} P_{ref,j} \quad (3.5)$$

Where M and N represent the number of direct paths from transmitters to a specific receiver and reflection paths to the same receiver,$P_{d,i}$ is received optical power from the i^{th} direct path and $P_{ref,j}$ is the received optical power from the j^{th} reflected path. The RMS delay spread is the critical performance criterion for the upper bound of the data transmission rate the mean excess delay is defined by

$$\mu = \frac{\sum_{i=1}^{M} P_{d,i}\, t_{d,i} + \sum_{i=1}^{N} P_{ref,j} t_{ref,j}}{P_{rT}} \quad (3.6)$$

And the RMS delay spread is given by

$$D_{RMS} = \sqrt{\mu^2 + (\mu)^2} \quad (3.7)$$

The distribution of mean delay spread, RMS delay spread D_{rms} which is the root mean square of the channel time delay and maximum achievable data rate. The maximum bit rate that can be transmitted through the channel without the need for an equalizer is given by

$Rb \leq 1/(10*\text{Drms})$.
(3.8)

3.1.2 Outdoor VLC System Model

Simulation a free space optical communication system featuring channel loss, pointing error, turbulence, fog/smoke condition comparing with all analytical solutions.

The system block diagram of the simulation procedure is illustrated in Figure 3.3.

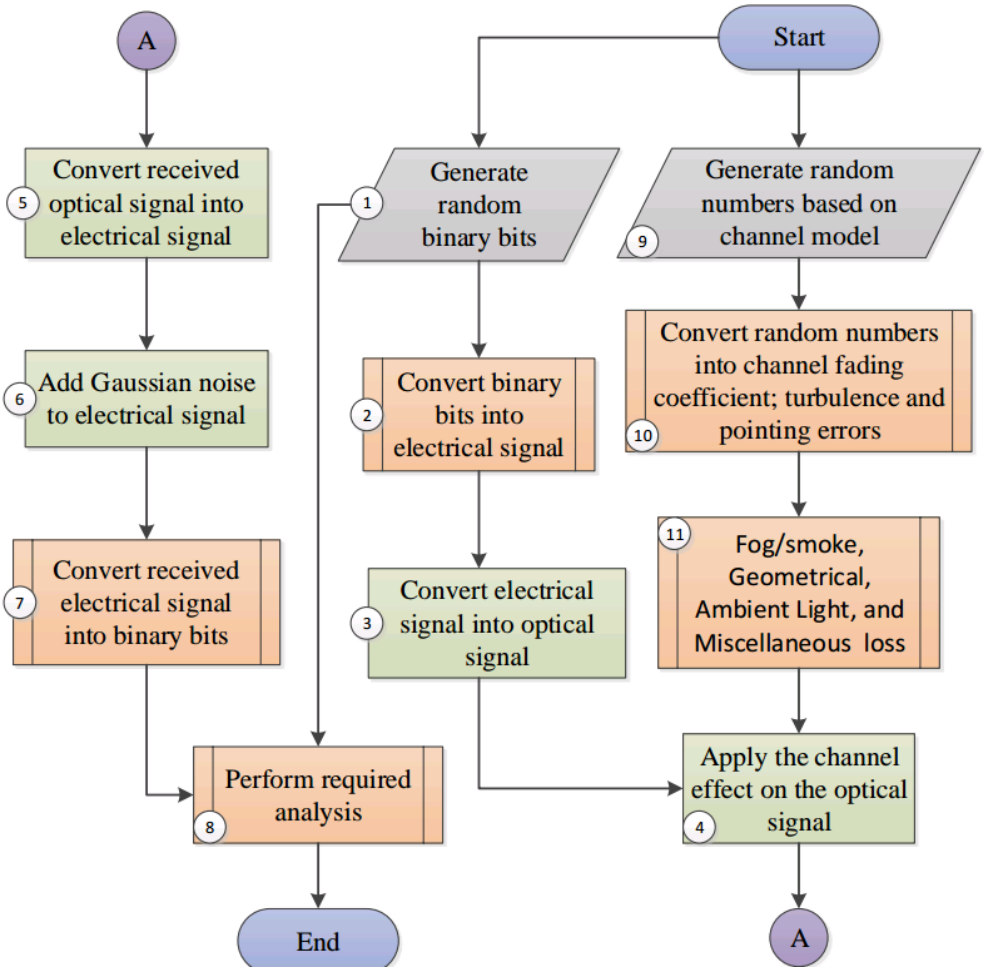

Figure 3.3 System block diagram of the simulation procedure

1 – Generating random binary bits

The random binary bits or pseudorandom binary sequence (PRBS) represent any random input data for the FSO system. These bits are generated using a uniform random number generator engine. MATLAB function: randi.

2 – Bit to electrical signal conversion

The generated bits $PRBS$ are resampled so that each bit is represented by NOS sample. MATLAB function: rectpulse. The value of NOS depends on the available memory and the time window over which the train is assumed stationary. Obviously for high data rates or slow trains, larger number of samples could be generated. If the train moves with the speed of v over the distance of Δl then it takes $T_{travel} = \Delta l/v$ to finish the travelling. If the baud rate is BR = $1/T_s$, where T_s is the symbol duration, then

$$NOS \leq \frac{Ttravel}{Ts} = \frac{\Delta l \times BR}{V} \tag{3.9}$$

3 – Electrical to optical signal conversion

Knowing the average output optical power P_{avg} and extinction ratio ε, the following equations are used to calculate the high and low powers corresponding to bits 1 and 0 when implementing OOK modulation:

$$p_{1} = \frac{2p_{avg}}{1+\frac{1}{\varepsilon}} \tag{3.10}$$

$$p_{0} = \frac{2p_{avg}}{1+\varepsilon} \tag{3.11}$$

$$\Delta p = P_1 - P_0 \tag{3.12}$$

By multiplying the generated electrical signal S_{elec} from step 2 by ΔP and adding the required optical power offset to accommodate the optical power average value, the optical signal at the transmitter side is generated

$\Delta P \times S_{elec} + P_{avg}$.

4 – Applying the channel effects

Once calculating the channel coefficients h, the optical power generated from step 3 is multiplied by the coefficients. The outcome is the optical received power at the receiver side. Depending on the simulation purpose, the coefficient h may be applied to varying optical signal P_{sig} or average optical power P_{avg} part. If calculating BER is the target of the simulation, the received signal is $h \times \Delta P \times S_{elec}$. However, if simulating a real system is desired the received signal would be $h \times (\Delta P \times S_{elec} + P_{avg})$.

5 – Optical to electrical signal conversion

To convert the received optical power to electrical signal, the responsivity of the photodiode as well as the TIA gain are used.

6 – Adding white Gaussian noise

If the SNR is given, by measuring the power of transmit signal in step 3, the required noise power P_n is calculated. To generate the additive noise, random numbers are generated based on random normal distribution N $(0,\sqrt{P_n})$. MATLAB function: randn.

7 – Bit extraction

A threshold level is set based on the average value of the received electrical signal. By comparing the midpoint of each received bit with the threshold, the received bit is determined to be 0 or 1. To perform adaptive thresholding, the length of averaging is changed from the whole received signal to smaller sections.

8 – Analysis

To perform the analysis, original transmit bits are compared to received bits, which leads to BER value. MATLAB function: biterr.

Another parameter extracted from the received signal is the Q-factor. Having the electrical signal level for bits 0 and 1, I can calculate Q-factor as

$$\text{Q-factor}=\frac{|V_1-V_0|}{\sigma_0-\sigma_1} \tag{3.13}$$

Where V_1 and V_0 are the mean values of received electrical signal corresponding to bits 1 and 0, respectively. While σ_1 and σ_0 are the standard deviation values of received electrical signal corresponding to bits 1 and 0, respectively.

The electrical SNR value is also calculated based on the signal power and existing noise power. From Section 3, the optical signal power is ΔP and at the receiver it results in voltage V_{sig} defined as

$$V_{sig} = G \times \eta \times \Delta \mathrm{p} \tag{3.14}$$

Where G, and η are transimpendace (TIA) gain, and responsivity, respectively.

Knowing the load impedance R_{load} the electrical signal power will be

$$P_{sig} = \frac{(G\times \mathrm{c}\times \Delta \mathrm{p})^2}{R_{load}} \tag{3.15}$$

If noise equivalent power (NEP) of the receiver is given and the signal bandwidth BW is known, the detector noise power is obtained as

$$P_{det} = NEP\sqrt{BW} \tag{3.16}$$

To take into account the background light and shot noise I have

$$i_n^2 = 2 \times q \times I \times BW \tag{3.17}$$

Where q is the electron charge and I is the induced current due to the noise. For background noise $I_{bg} = \eta P_{bg}$, where P_{bg} is the background illumination power. In case of shot noise, if the received average optical power is P_r then $I_{sn} = \eta P_r$. Finally the noise power at the output of TIA will be

$$P_n = \frac{2q\eta G^2 BW}{R_{load}}(P_{bg} - P_r) \tag{3.18}$$

And the total noise power will be

$$P_{noise} = NEP\sqrt{BW} + \frac{2q\eta G^2 BW}{R_{load}}(P_{bg} - P_r) \tag{3.19}$$

9 – Generating random number for channel fading

Based on the fading type, different kinds of random numbers are generated. In our simulation, turbulence and pointing errors are random phenomena. Different models are used to generate channel coefficient for each. I will briefly explain each process below

A- Turbulence, Log-Normal model

$$x = N(\mu_{x,turb}, \sigma_{x,turb}) \tag{3.20}$$

$$h_{t-LN} = \exp(2X) \tag{3.21}$$

MATLAB function: randn.

B- Turbulence, Gamma-Gamma model

$$X = \Gamma(\alpha, 1) \tag{3.22}$$

$$Y = \Gamma(\beta, 1)$$

(3.23)

$$h_{t-GG} = \frac{1}{\alpha\beta} XY \tag{2.24}$$

MATLAB function: gamma

C-Pointing error, Log-Normal-Rician model

$$X = N(\mu_{x,PE}, \sigma_{j,PE}) \tag{3.25}$$

$$Y = N(\mu_{y,PE}, \sigma_{j,PE}) \tag{3.26}$$

$$r = \sqrt{X^2 + Y^2} \tag{2.27}$$

$$h_{PE} = A_0 \exp\left(-\frac{2r^2}{w^2{}_{eq}}\right) \tag{3.28}$$

10 – Generating channel coefficient for turbulence and pointing errors

Once the values are generated, they are resampled to simulate the proper channel effect. If the bit rate is DR after resampling the bits in step two, the sampling frequency will be $F_s = DR \times NOS$. Typical channel temporal coherence for turbulence and pointing error is 1 – 1 msec. I pick F_{fading} = 500 Hz for our work. These values are used to resample fading effects to fit the whole signal. Two possible options exist to do resampling, either doing staircase resampling or resampling by using polyphaser anti-aliasing filter. MATLAB functions: rectpulse, and resample.

To confirm each model, the simulation results are compared with the available theory.

BER in clear channel

$$BER = Q\left(\frac{\eta \mathrm{I_o}}{\sqrt{2N_o}}\right) \tag{3.29}$$

Where

$$Q(x) = \frac{1}{2\pi}\int_x^\infty \exp(-\frac{u^2}{2})du \; is \; Q \; function. \tag{3.30}$$

BER in pointing errors channel

$$BER = \exp\left(-\frac{s^2}{s\sigma_s^2}\right)\sum_{i=1}^{k} w_i Q[\frac{\eta I_o A_o}{\sqrt{2N_o}}\exp\left(-\frac{4\sigma_s^2}{w_{eq}^2}x_i\right) I_o(s\sqrt{\frac{2x_i}{\sigma_s^2}}]$$

(3.31)

It is based on Gauss-Lagurerre quadrature formula (refer to Appendix A from Doc-F02-D2). $I_o(\cdot)$ is zero-th order modified Bessel function of first kind. [2] is used for PDF.

BER in turbulence channel – Log-Normal model

$$\text{BER} = \exp\left(-\frac{s^2}{s\sigma_s^2}\right)\sum_{i=1}^{k} w_i Q[\frac{\eta I_o A_o}{\sqrt{2N_o}}\exp\left(-\frac{4\sigma_s^2}{w_{eq}^2}x_i\right) I_o(s\sqrt{\frac{2x_i}{\sigma_s^2}} \qquad (3.32)$$

It is based on Gauss-Hermite quadrature formula

BER in turbulence channel – Gamma-Gamma model

$$BER = \frac{2^{\alpha+\beta-3}}{\sqrt{\pi^3}l(\alpha)l(\beta)} G_{5,2}^{2,4}\left(\frac{2}{\alpha\beta}\right)^2 \times 2 \times \frac{\eta\, I_o}{\sqrt{2N_o}}\left|\frac{1-\alpha}{2}, \frac{2-\alpha}{2}, \frac{1-\beta}{2}, \frac{2-\beta}{2}, 1\right| \qquad (3.33)$$

Where ${G_{5,2}}^{2,4}[\cdot]$ is Meijer's G function [3].

BER in pointing errors and turbulence channel – Log-Normal model

$$\text{BER}=\frac{2\gamma^{2-1\left(\frac{\gamma^2}{2}+\frac{1}{2}\right)exp\left(\frac{s^2}{\sigma_s^2}+2\sigma_x^2\gamma^2+2\sigma_x^2\gamma^4\right)}}{\sqrt{\pi(A_0)}} \times \left(\frac{I_0}{\sqrt{2N_0}}\right)^{\frac{\gamma^2}{2}} \qquad (3.34)$$

This BER formula is an asymptotic .approximation for large SNR values [2].

BER in pointing errors and turbulence channel – Gamma Gamma model

BER =

$$\frac{2^{\beta-1}\Gamma\left(\frac{\beta}{2}+\frac{1}{2}\right)exp\left(\frac{s^2}{2\sigma_S^2}+\frac{\frac{-s^2\gamma^2}{\sigma_S^2}}{2\beta-2\gamma^2}\right)}{\Gamma(\alpha)\Gamma(\beta)sin[(\alpha-\beta)\pi]\Gamma(-(\alpha-\beta)+1)|\gamma^2-\beta|\beta}\Gamma\left(\frac{\beta+1}{2}\right)\sqrt{\pi\gamma^2}\left(\frac{I_0}{\sqrt{2N_0}}\right)^{-\beta/2} \quad (3.35)$$

This BER formula is an asymptotic .approximation for laRge SNR values [2].

In case, the receiver has an aperture with diameter of d_s then for Gamma-Gamma model the parameters will be

$$K = \frac{2\pi}{\gamma} \quad (3.36)$$

$$D = \left(kd_s^2/4L\right)^{0.5} \quad (3.37)$$

$$\sigma^2 LnX = \frac{0.49\sigma_R^2}{\left(1+0.65d^2+1.11\sigma_R^{12/5}\right)^{7/6}} \quad (3.38)$$

$$\sigma^2 LnX = \frac{0.51\sigma_R^2(1+0.69\sigma_R^{12/5})^{-5/6}}{1+0.90d^2+0.62d^{2\sigma_R^{12/5}}} \quad (3.39)$$

For Log-Normal model, it is given as

$$\frac{\sigma_I^2(d_s)}{\sigma_I^2(0)} \approx [1+1.062d^2]^{-7/6} \quad (3.40)$$

11 – Fog/smoke loss

Based on the visibility Vis and by using Kim model, q parameter is defined

$$q = \begin{cases} 1.6, & Vis > 50 \\ 1.3, & 6 < Vis < 50 \\ 1.6 \times Vis + 0.34, & 1 < Vis < 6 \\ Vis - 0.5, & 0.5 < Vis < 0.1 \\ 0, & Vis < 0.1 \end{cases} \quad (3.41)$$

Having the laser wavelength λ (nm), the parameter β_λ in $1/km$ is defined as

$$\beta_\lambda = -\frac{ln0.02}{Vis}\left(\frac{\gamma}{550}\right)^{-q} \quad (3.42)$$

And finally by using Beer's lambert law, the fog/smoke loss will be

$$h_{Fs} = \exp(-\beta_\lambda L) \quad (3.43)$$

Where L is the link distance in km.

12 – Geometrical loss

Geometrical or propagation loss for the elliptical beam is estimated based on the followings:

• Receiver aperture to source L distance $\gg \lambda$

• Receiver aperture area $A_{RX-apr} \ll$ beam size at receiver aperture plane W (Z)

The geometry of the beam and receiver is considered the same as Figure 3.4

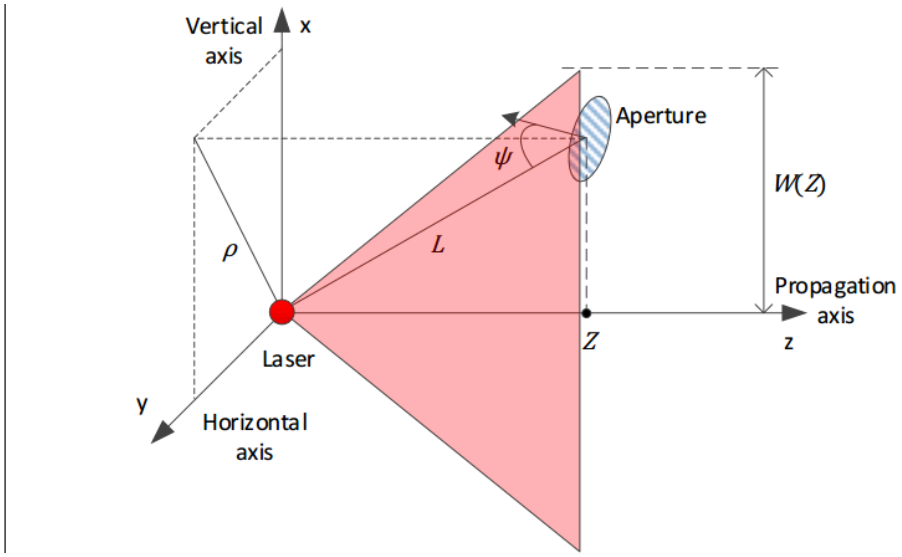

Figure3.4 laser beam and receiver aperture geometry

The geometrical loss of the aperture while the normalized intensity $I_n(\rho; z)$is given will be:

$$h_{GL} = I_n(\rho; Z) \times T_r A_{Rx-apr} \times \cos\Psi, \quad \Psi \leq \frac{1}{2} AFOV \tag{3.44}$$

Where AFOV and T_r are full-angle angular field-of-view, and transmittance of the receiver aperture. The angle ψ is defined as the angle between the vector connecting laser to the aperture and the vector normal to the aperture. I consider two radiation mechanism for the source, uniform and Gaussian. If the laser is a multimode-propagation source, it can be approximated with a uniform pattern. Otherwise a Gaussian propagation is considered.

A-Uniform radiation: when the intensity of the laser beam is uniform across the wave front.

$$I_n(\rho; Z) = \frac{1}{\pi \times w_h(Z) \times w_v(Z)} \tag{3.45}$$

Where P_{Tx} is the total power of the beam; $w_h\ (Z)$ and $w_v(Z)$ are beam radius along horizontal and vertical directions, respectively.

$$W_h(Z) = w_{Oh} + Z\theta_{Oh} \tag{3.46}$$

$$W_V(Z) = w_{Ov} + Z\theta_{Ov} \quad (3.47)$$

w_{oh} and w_{ov} are beam radii at transmitter side along horizontal and vertical directions, respectively. θ_{oh} and θ_{ov} are beam divergence (1/e criterion) at transmitter side along horizontal and vertical directions, respectively.

B-Gaussian radiation: the intensity profile is Gaussian.

$$\mathrm{I_n(p;z)} = \frac{2}{\pi \times w_h(Z) \times W_{V(Z)}} \exp\left(-\frac{2X^2}{W_V(Z)^2} - \frac{2y^2}{w_h(Z)^2}\right) \quad (3.48)$$

$$W_h(Z) = w_{Oh}\sqrt{1 + \varepsilon_h\left(\frac{\gamma Z}{\pi w o h^2}\right)^2} \quad (3.49)$$

$$W_v(Z) = w_{Ov}\sqrt{1 + \varepsilon_v\left(\frac{\gamma Z}{\pi w o v^2}\right)^2} \quad (3.50)$$

$$\varepsilon h = 1 + 2\frac{wov^2}{P_{0(Z)^2}} \quad (3.51)$$

$$\varepsilon_v = 1 + 2\frac{\mathrm{woh^2}}{\mathrm{P_{0(Z)^2}}} \quad (3.52)$$

$$p_0(z) = (0.55cn^2k^2Z)^{-\frac{3}{2}} \quad (3.53)$$

3.2 Performance Metrics

3.2.1 Indoor VLC system Performance Metrics.

The performance metrics that will study as Received Signal Strength (RSS), Signal to Noise Ratio (SNR), and delay.

3.2.2 Outdoor VLC system Performance Metrics.

PDF-XChange Editor
Click to BUY NOW!
www.tracker-software.com

The performance metrics that will study as Bit Error Rate (BER) with Signal to Noise Ratio under different loss such as fog, smoke, turbulence, geometrical loss, and pointing error.

CHAPTER FOUR

SIMULATION AND RESULT

This chapter presents a part of the simulation results obtained by running the MATLAB code program. The results include the performance metrics like: RSS, SNR, delay spread in different angles with change in space for (MIMO) scenario in indoor VLC system and SNR Vs BER in outdoor VLC system.

4.1 Simulation Description

In indoor system we assumed the room center is 0 and -4 at the left side 4 at the right side in the x and y axis, and the parameters are shown in the table 4.1, and table 4.2 shown the parameters in outdoor VLC system.

Table 4.1 Simulation parameters for indoor VLC system

Parameters	Value
Size	**8 × 8 × 3 m3**
Reflection coefficient	0.8
angle at half power	**60°**
Transmitted power (per LED)	20 mw
Number of LEDs per array	**60 × 60 (3600) LEDs**
Receive plane above the floor	0.85m
Half-angle FOV	**75°**

Table 4.2 Simulation parameters for outdoor VLC system

Full vertical divergence angle(TX)	10°
horizontal divergence angle(TX)	10°
Source Cartesian position	0,0,0
Receiver aperture diameter	0,005 m
Receiver aperture transmitter	85%
FOV	1°

4.2 Result and Discussion

4.2.1 Result and Discussion for indoor VLC system

The optical power distribution at receiver plane in a LOS path (ignoring the reflection of walls)**.** Figure 4.1 show it can be seen that there is almost uniform distribution of optical power at the room area with a maximum -8 dB and minimum power -60 dB at half angle 15°.

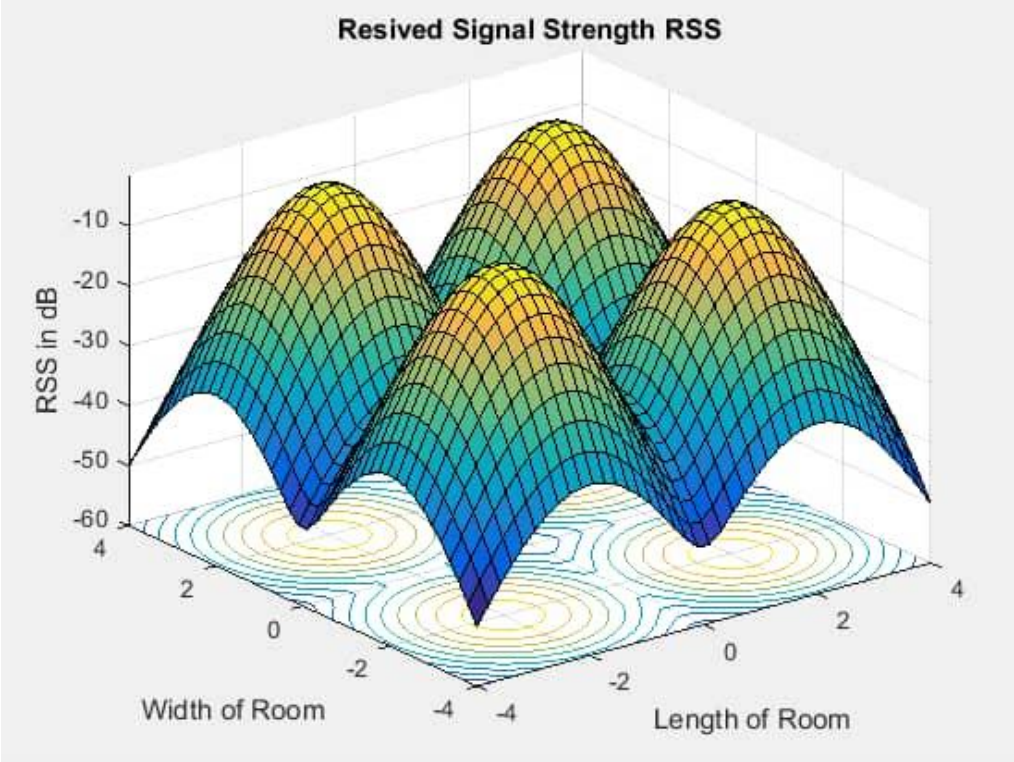

Figure 4.1 power received signal strength at15°.

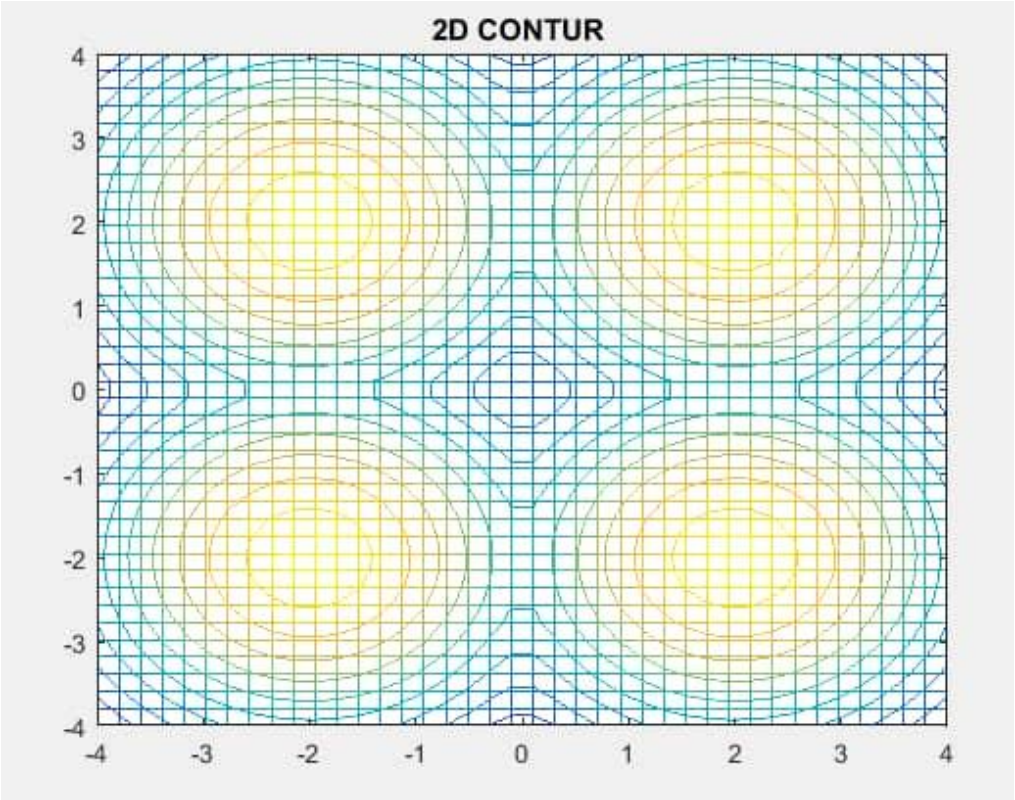

Figure 4.2 contour received signal at 15°

Figure 4.3 show distribution of optical power at the room area at half angle 30° with a maximum -10 dB and minimum power -25 dB.

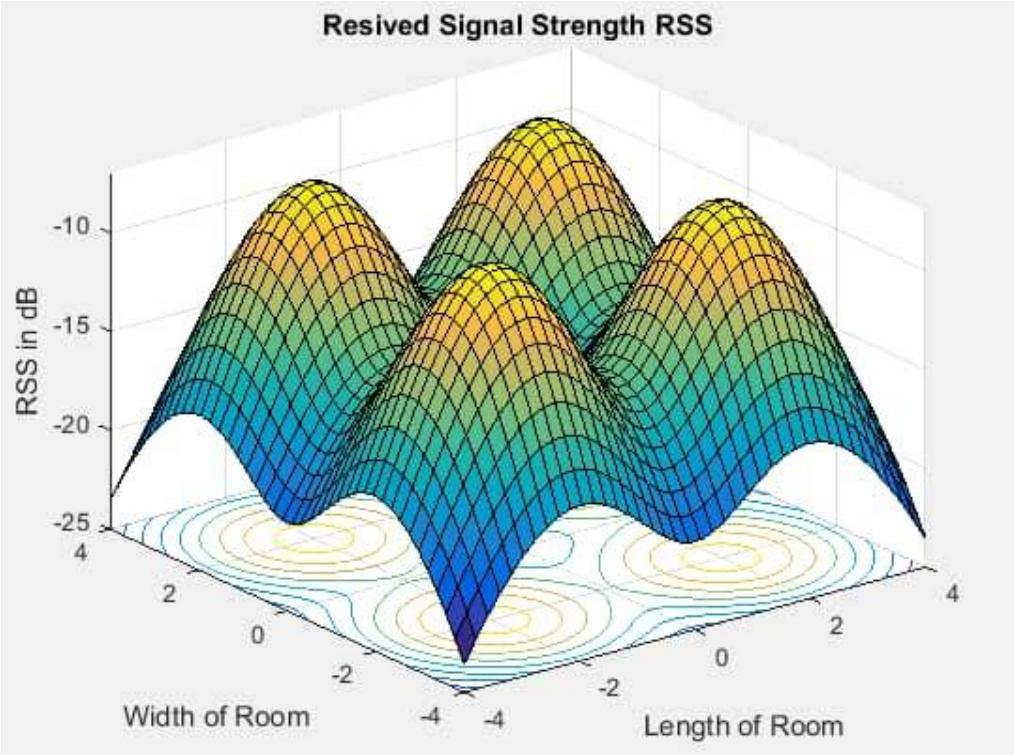

Figure 4.3 power received signal strength at30°.

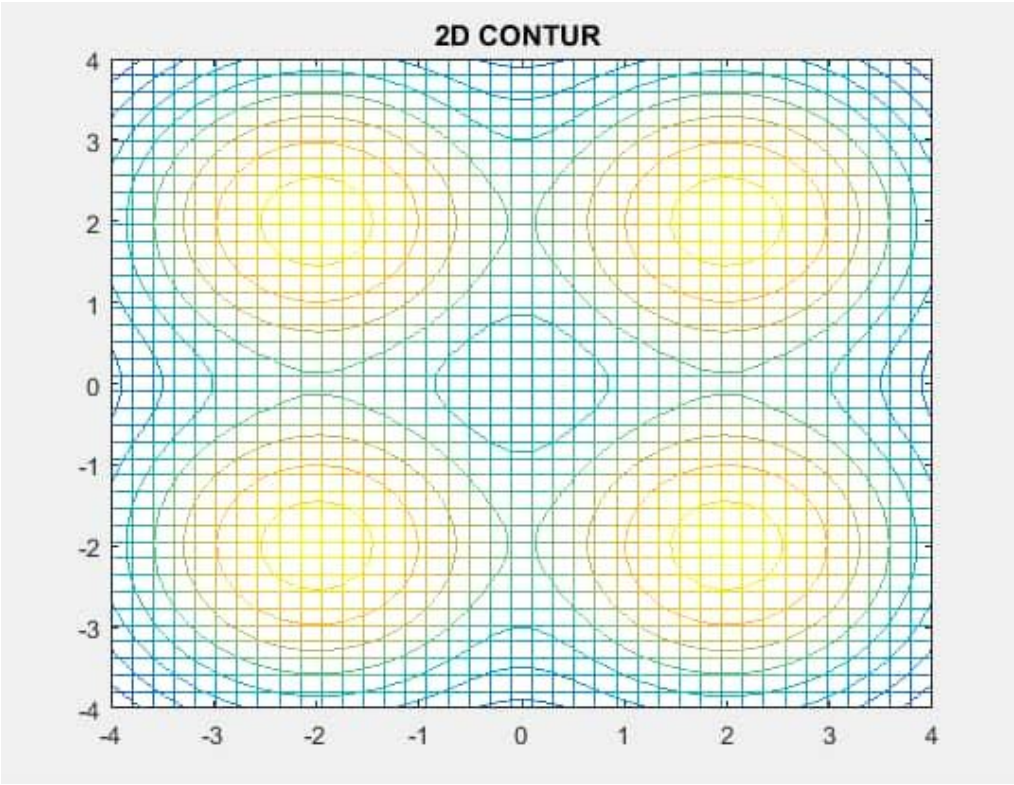

Figure 4.4 power received signal strength at30°.

Figure 4.5 show distribution of optical power at the room area at half angle 60° with a maximum -2 dB and minimum power -10 dB .

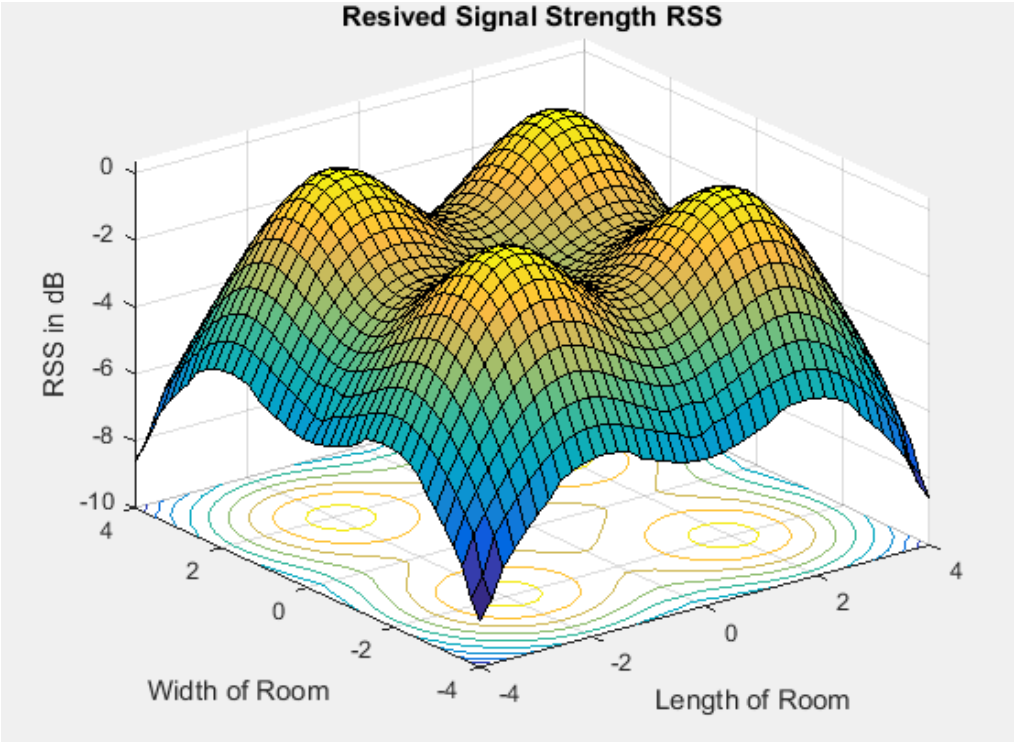

Figure 4.5 power received signal strength at60°.

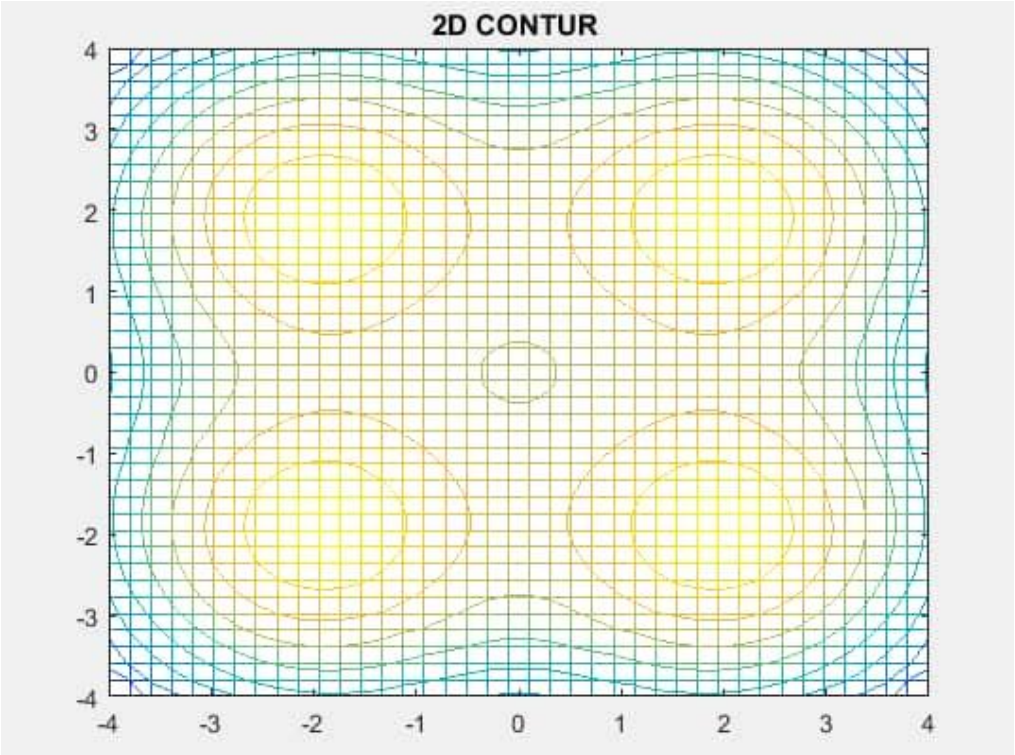

Figure 4.6 power received signal strength at60°

As the angle value increases, the Received Signal Strength decreases.

Contour LED illuminance distribution is show in figure 4.2, figure 4.4 and figure 4.6 it can be seen that there is improvement the coverage area at half angle 15 and half angle 30 than half angle 60.

4.2.1.2 Signal to Noise Ratio result

The Figure 4.7 shows the signal to noise ratio (SNR) the system model at half angle 15°is fluctuated between 40 dB and110 dB.

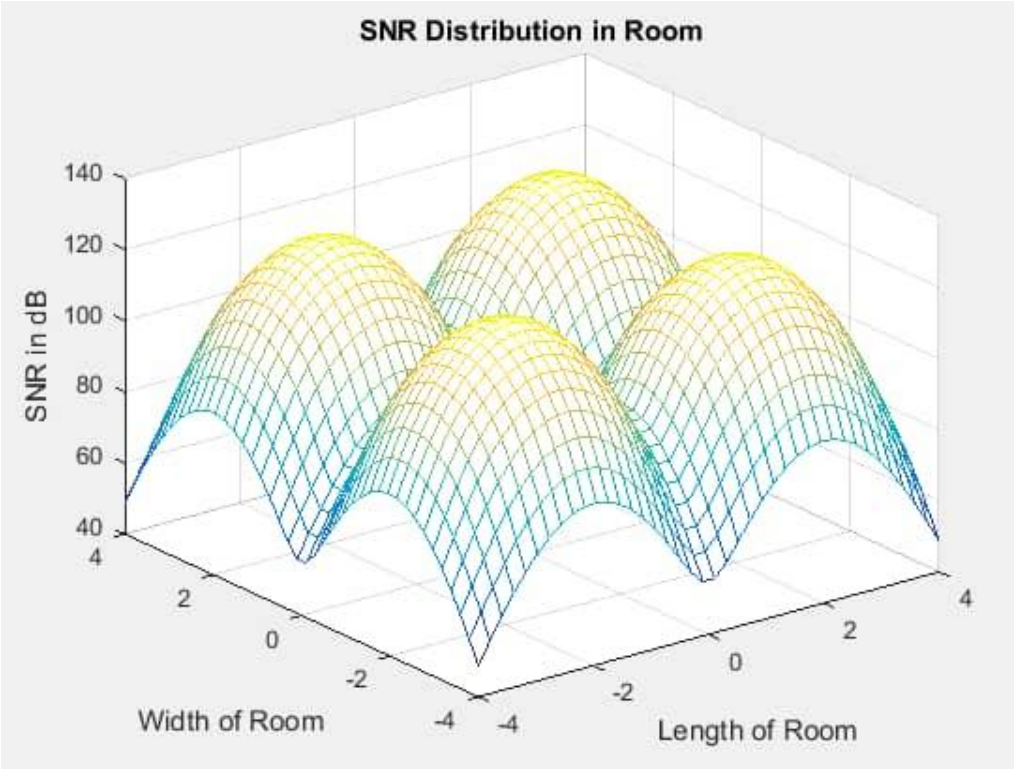

Figure 4.7 Signal To Noise Ratio at 15°.

The Figure 4.8 shows the signal to noise ratio (SNR) the system model at half angle 30°is fluctuated between95 dB and115 dB.

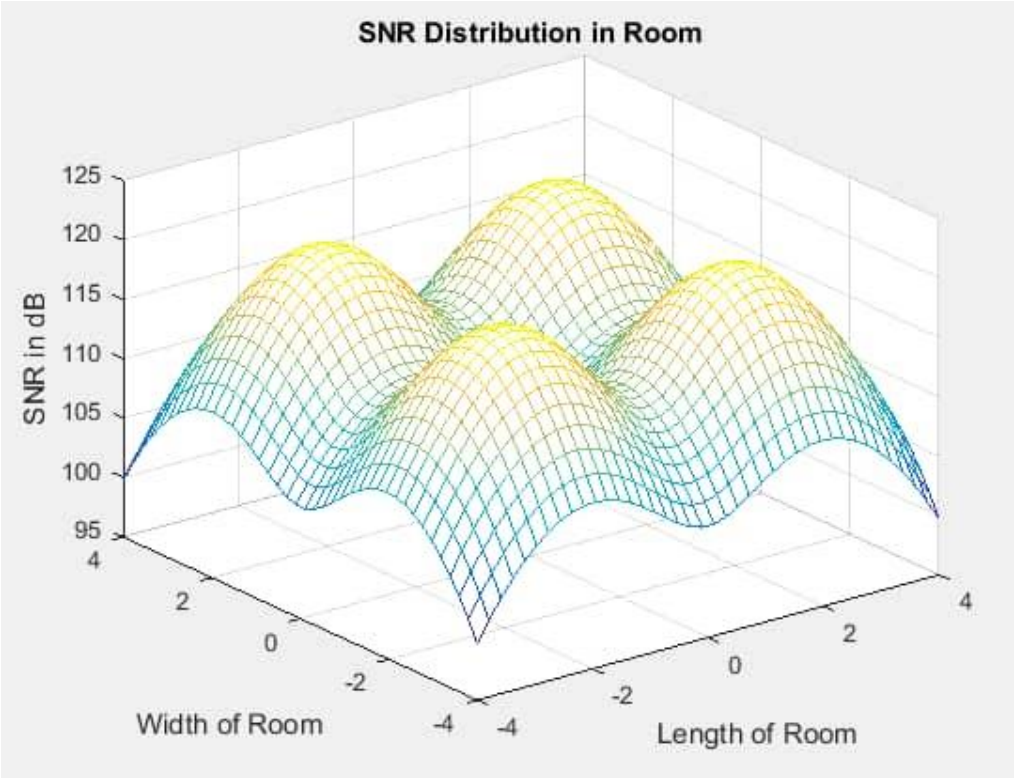

Figure 4.8 signal to noise ratio at 30°.

The Figure 4.9 shows the signal to noise ratio (SNR) the system model at half angle $60^{\circ}$is fluctuated between118 dB and126 dB.

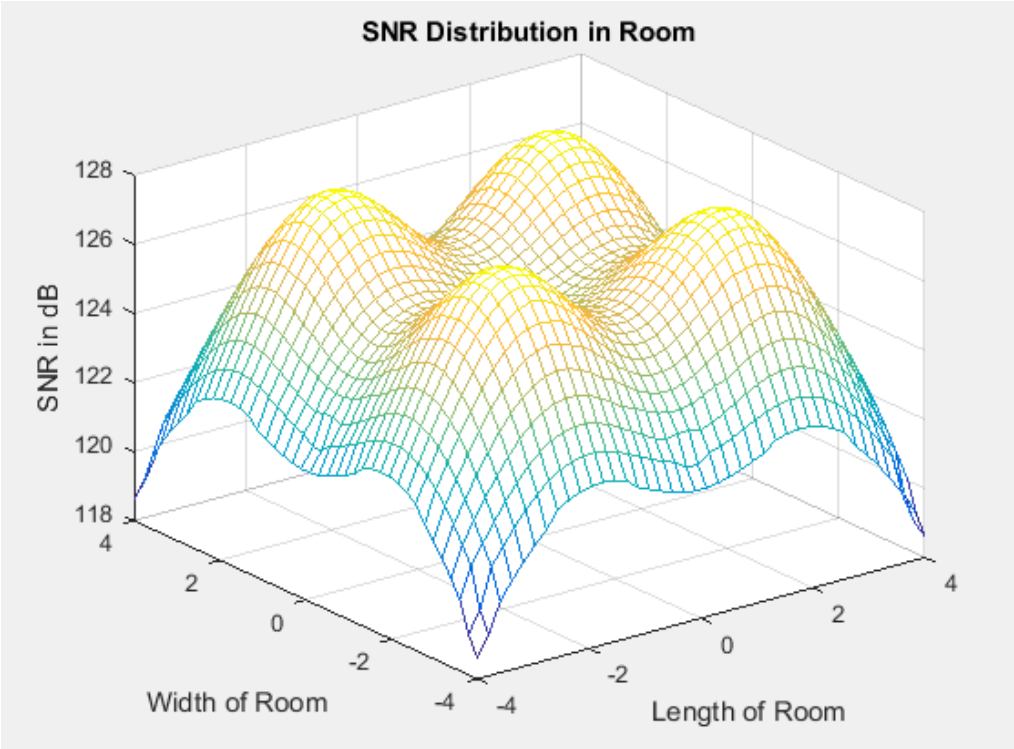

Figure 4.9 signal to noise ratio at 60°.

Comparison between half angles 15°, 30°,60°SNR is decrement at half angle 15 and improving at half angle 60.

4.2.1.3 Delay results

The RMS delay spread distribution at half angle 15° Figure 4.10 show the maximum and average range values for this case are 0.05ns and0.025ns, respectively.

Thus the maximum achievable data rate in diffuse channel is 2000 Mbps.

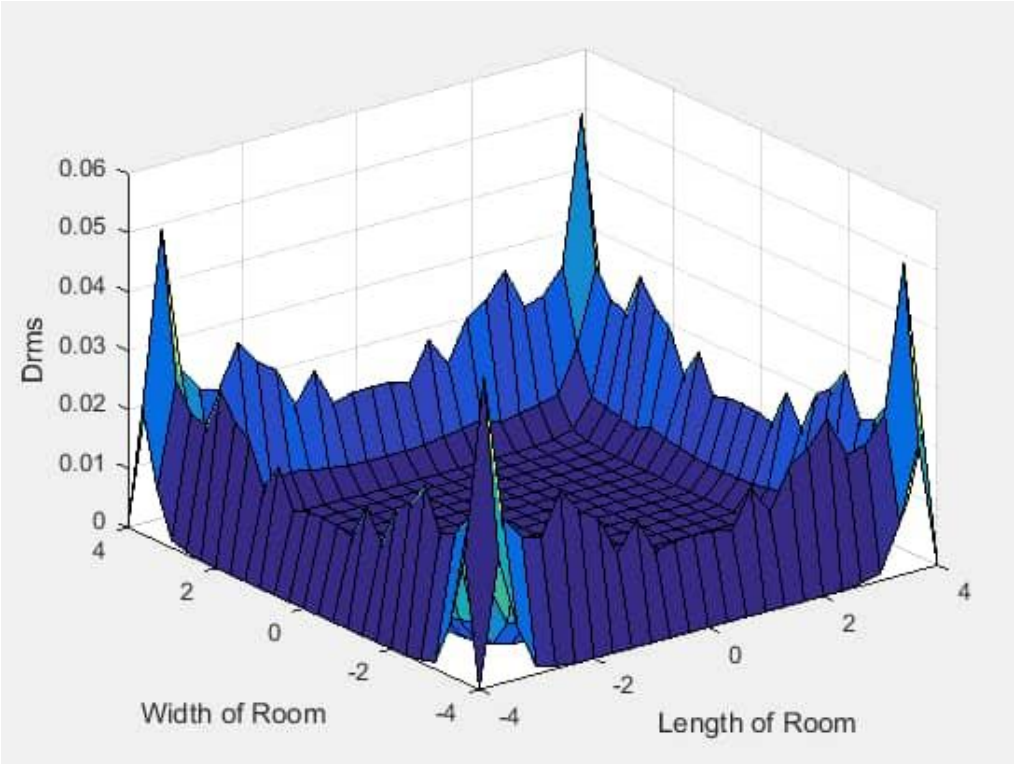

Figure 4.10 delay root mean square at 15°.

Figure 4.11 show at half angle $30^{\circ}$the maximum and average range values for this case are 0.3ns and0.15ns, respectively.

Thus the maximum achievable data rate in diffuse channel is

333 Mbps.

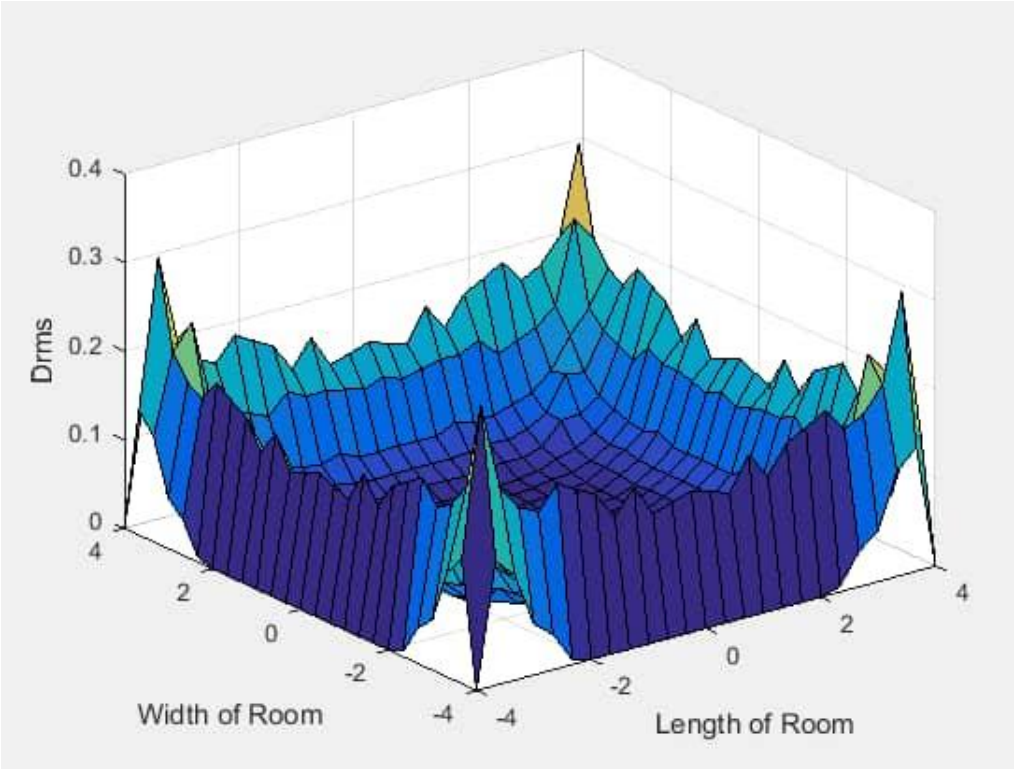

Figure 4.11 delay root mean square at 30°.

Figure 4.12 show at half angle $60^{\circ}$the maximum and average range values for this case are 0.6ns and0.3ns, respectively.

Thus the maximum achievable data rate in diffuse channel is

166 Mbps.

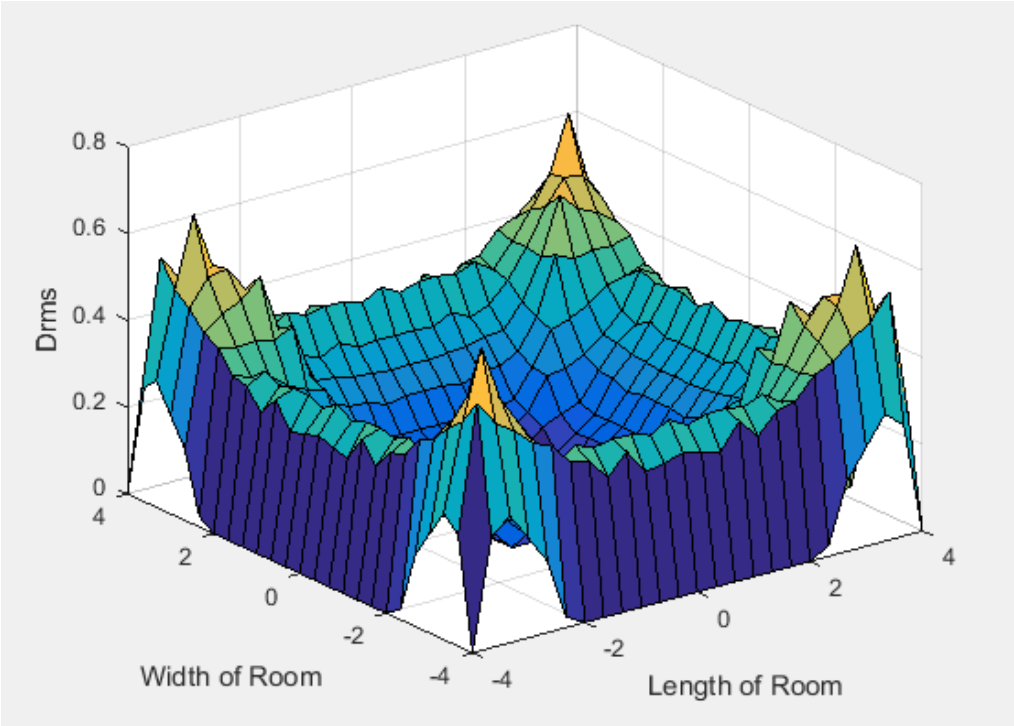

Figure 4.1 delay root mean square at 60°.

As the half angle value increases, the delay RMS increases

4.2.2 Result and Discussion for outdoor VLC system

Figure 4.13 show when signal to noise ratio (SNR) was in its minimum value the bit error rate (BER) increase and vice versa, and compare between simulation and theoretical.

When average optical power equal -10.000 dBm, 0.100 mW and SNR equal 5.64 dB, simulation BER equal 0.137 and theoretical BER equal 0.138.

When average optical power equal 6.990 dBm, 5.000 mW and SNR equal 39.62 dB, simulation BER equal 0.000484 and theoretical BER equal 0.00035.

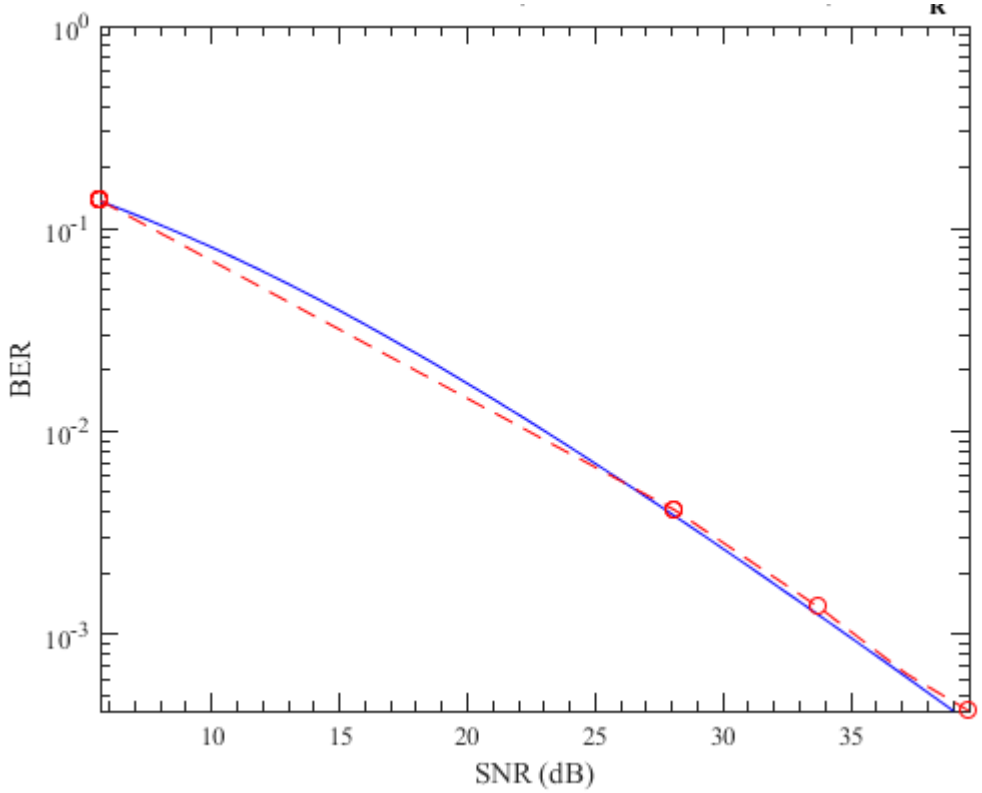

Figure 4.13 BER vs. SNR for turbulence channel

Figure 4.14show change in curve between SNR and BER.

When average optical power equal -10.000 dBm, 0.100 mW and SNR equal 5.64 dB, simulation BER equal 0.0279 and theoretical BER equal 0.0279.

When SNR more than 5.64 BER is approximately zero.

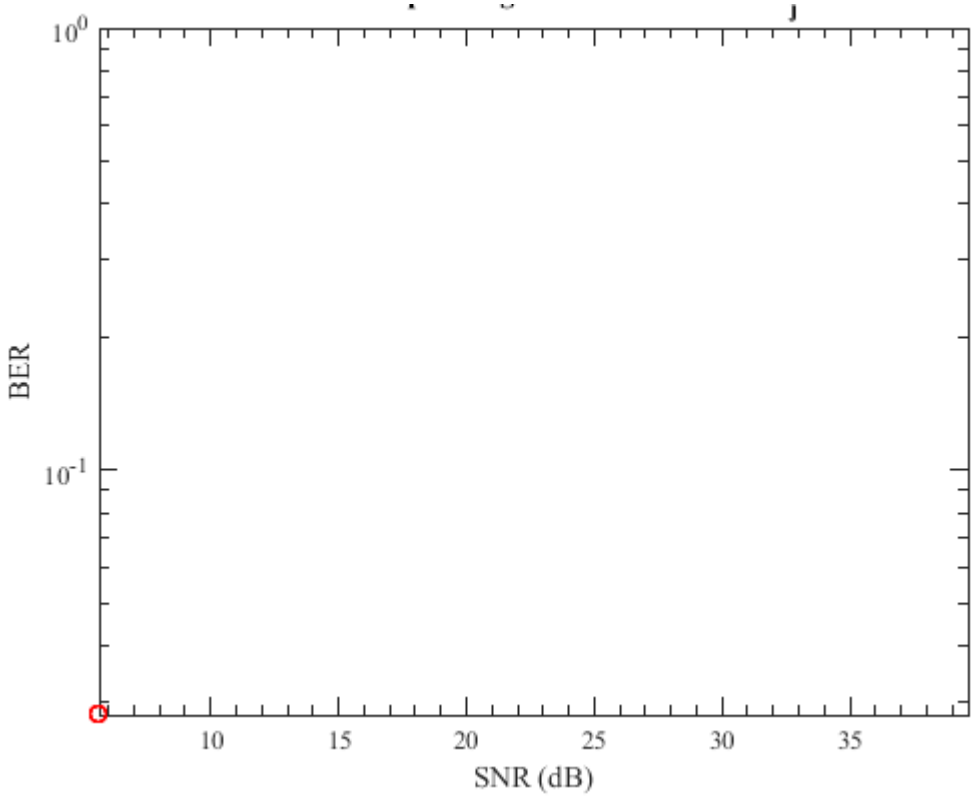

Figure 4.14 BER vs. SNR for pointing error channel

Figure 4.15 show change in curve between SNR and BER.

When average optical power equal -10.000 dBm, 0.100 mW and SNR equal -1.92 dB, simulation BER equal 0.212 and theoretical BER equal 0.212.

When SNR more than 28 BER is approximately zero.

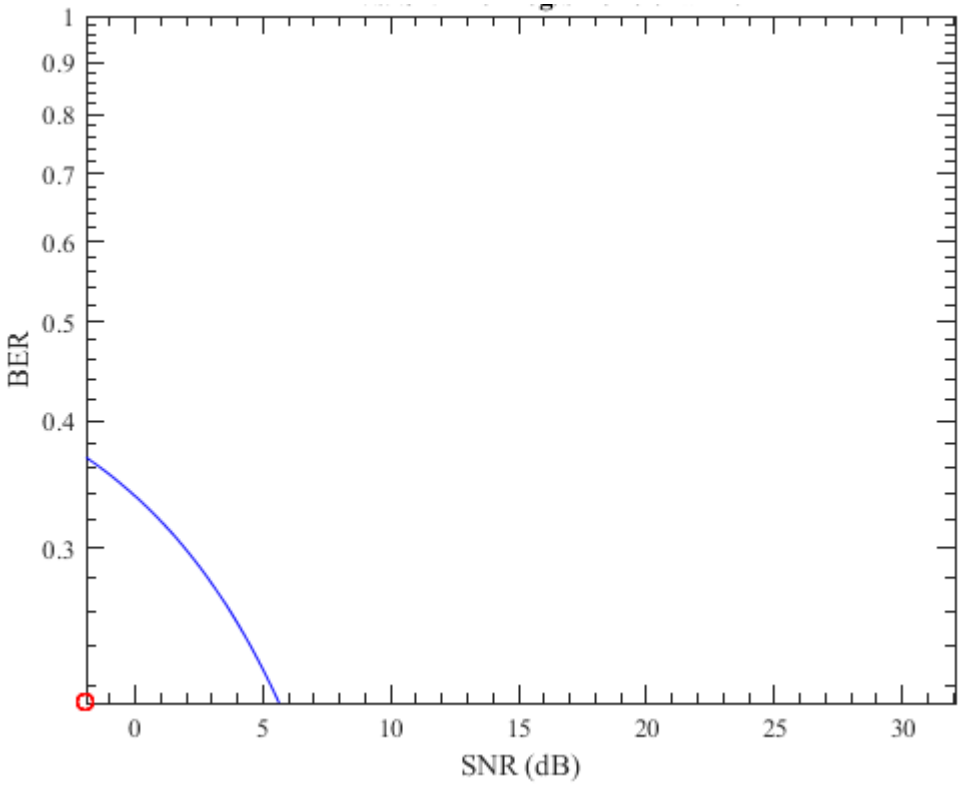

Figure 4.15 BER vs. SNR for fog/smoke

CHAPTER FIVE

CONCLUSION AND RECOMMENDATION

5.1 Conclusion

To evaluating the performance for indoor VLC channel, proposed system is mathematically analyzed and simulated against the various quality of transmission parameters such as Received signal strength (RSS), Signal to Noise Ratio (SNR), and propagation delay, and bit error rate Compare with signal to noise ratio in outdoor VLC system. The quality of transmission is evaluated by measuring the received signal strength, signal to noise ratio and delay under different half angles (15°, 30°, 60°).

The result showing receive signal strength is the best at angle 15° while the signal to noise ratio analysis decrement at the same angle but improve at half angle 60°, and RMS delay increases with increasing angles.

The quality of transmission is evaluated by measuring (BER vs. SNR) under various channel effect turbulence channel, pointing error and fog/smoke. minimum (BER) result with effect of smoke/fog was better than another effect of different losses outdoor VLC system.

5.2 Recommendation

Proposed system can mathematically analyze and simulate the various parameter and quality of transmission in (SISO) scenario for indoor VLC channel model and different losses outdoor channel for

PDF-XChange Editor
Click to BUY NOW!
www.tracker-software.com

example evaluate the performance for channel under effect of snow and rain.

Reference

[1] Zabih Ghassemlooy, Luis Nero Alves, Stanislav Zvánovec, Mohammad-Ali Khalighi "Visible Light Communications Theory and Applications" England 2017.

[2] Z.Ghassemlooy, W.Popoola, S.Rajbhandari "Optical Wireless Communication"Channel Modelling with MATLAB, Taylor&Francis Group,(2013)

[3] Pranav Kumar Jha, Neha Mishra, and D. Sriram Kumar "Challenges and potentials for visible light communications: State of the art" American Institute of Physics 2017.

[4] Yang Qiu1, Hsiao-Hwa Chen2* and Wei-Xiao Meng1 Channel modeling for visible light communications—a survey

[5] Prabu Subramani , Ganesh Babu Rajendran , Jewel Sengupta , Rocío Pérez de Prado,and Parameshachari Bidare Divakarachari "A Block Bi-Diagonalization-Based Pre-Coding for Indoor Multiple-Input-Multiple-Output-Visible Light Communication System" 2020.

[6] Farshad Miramirkhani1 andMuratUysal2 "channel modeling for indoor visible light communications" Turkey 2020.

[7] Sheng-HongLin1, 2,ChengLiu3, XuBao 1 andJin-YuanWang1 "Indoor visible light communications: performance evaluation and optimization" EURASIP Journal on wireless communication and networking 2018.

[8] Sheng-HongLin1, 2 ,ChengLiu3, XuBao 1 andJin-YuanWang1 "Indoor visible light communications: performance evaluation and optimization" EURASIP Journal on wireless communication and networking, (2018).

[9]Reham W. Zaki, Heba A. Fayed, Ahmed Abd El Aziz and Moustafa H. Aly, Outdoor Visible Light Communication in Intelligent Transportation Systems: Impact of Snow and Rain, Egypt, 12 December 2019.

[10]Véronique Georlette 1 , Sébastien Bette 2, Sylvain Brohez 3, Rafael Pérez-Jiménez 4 , Nicolas Point 5 and Véronique Moeyaert , Outdoor

PDF-XChange Editor Click to BUY NOW! www.tracker-software.com

Visible Light Communication Channel Modeling under Smoke Conditions and Analogy with Fog Conditions, Belgium, 2020.

[11]Alin Cailean, Barthélemy Cagneau, Luc Chassagne, Valentin Popa, Mihai Dimian, Evaluation of the noise effects on visible light communications using Manchester and Miller coding, Suceava,Romania,2015.

[12]Elizabeth Eso 1, Zabih Ghassemlooy 1 , Stanislav Zvanovec 2 , Juna Sathian 1, Mojtaba Mansour Abadi 1 and Othman Isam Younus, Performance of Vehicular Visible Light Communications under the Effectsof AtmosphericTurbulence withAperture Averaging, China,2021.

[13] Jie Lian1, Zafer Vatansever1, Mohammad Noshad2 and MaïtéBrand ” Indoor visible light communications, networking, and applications”

[14] P. A. Haigh, Z. Ghassemlooy, H. Le Minh, S. Rajbhandari, F. Arca, S. F. Tedde, O. Hayden, and I. Papakonstantinou. Exploiting equalization techniques for improving data rates in organic optoelectronic devices for visible light communications.J. LightwaveTechnol, 2012

[15] S. T. Le, T. Kanesan, F. Bausi, P. A. Haigh, S. Rajbhandari, Z. Ghassemlooy, I. Papakonstantinou, et al. 10 Mb/s visible light transmission system using apolymer light-emitting diode with orthogonal frequency division multiplexing. 2014.

[16] J. H. Burroughes, D. D. C. Bradley, A. R. Brown, R. N. Marks, K. Mackay, and R. H. Friend. Light-emitting diodes based on conjugated polymers. Nature, 1990.

[17] O Bouchet, M El Tabach, M Wolf, D C O’Brien, G E Faulkner, J W Walewski, S Randel,”Building the next-generation home network, 6th International Symposium on Communication Systems, Networks and Digital Signal Processing”, Austria, 2008

[18] M A Naboulsi, H Sizun and F d Fornel,” Wavelength selection for the free space optical telecommunication technology”, 2004

PDF-XChange Editor
Click to BUY NOW!
www.tracker-software.com

[19] Professor Z. Ghassemlooy, Dr. W. Popoola, Dr. S. Rajbhandari,"Optical Wireless Communications System and Channel Modelling with MATLAB",2009

[20] W Binbin, B Marchant and M Kavehrad, "Dispersion analysis of 1 55 μm free space optical communications through a heavy fog medium", IEEE Global Telecommunications Conference, Washington, USA, 2007

Appendix A (indoor VLC system model)

```
disp('indoor VLC LOS channel witZh RSS &Drms& SNR parameters')
lx=8; ly=8; lz=3;% office dimension in meter
h=2.2; %the distance between source and receiver plane
Rb = 1e6;                    % Data rate of system
I2 = 0.562;                  % Noise Bandwidth Factor
Iamp = 5e-12;                % Amplifier Current
Bn = 50e6;                   % Noise Bandwidth
R = 1;                       % Responsivity of Photodiode
q = 1.6e-19;                 % Electron Charge
[XT,YT]=meshgrid([-lx/4 lx/4],[-ly/4 ly/4]);
x=linspace(-lx/2,lx/2,lx*5);
y=linspace(-ly/2,ly/2,ly*5);
[XR,YR]=meshgrid(x,y);
P_LED=4e-3; %transmitted optical power by individual LED
nLED=16; % number of LED array nLED*nLED
P_total=nLED*nLED*p_LED; %Total transmitted power
theta = 60 ;  % semi-angle at half power
ml=-log10(2)/log10(cosd(theta)); %Lambertian order of emission
Adet=.4; %detector physical area of a PD
Ts=1;%gain of an optical filter
index=1.5;%refractive index of a lens at a PD
FOV=70;%FOV of a receiver
G_Con=(index^2)/(sind(FOV).^2);%gain of an optical concentrator
D1=sqrt((XR-XT(1,1)).^2+(YR-YT(1,1)).^2+h^2);% distance vector from
%source 1
cosphi_A1=h./D1;% angle vector
receiver_angle=acosd(cosphi_A1);
H_E1=(ml+1)*Adet.*cosphi_A1.^(ml+1)./(2*pi.*D1.^2);% channel DC
%gainforsource 1
P_rec_E1=P_total.*H_E1.*Ts.*G_Con;% received power from source 1;
P_rec_E1(abs(receiver_angle)>FOV)=0;
P_rec_E2=fliplr(P_rec_E1);
P_rec_E3=flipud(P_rec_E1);
P_rec_E4=fliplr(P_rec_E3);
P_rec_total=P_rec_E1+P_rec_E2+P_rec_E3+P_rec_E4;
P_rec_dBm=pow2db(P_rec_total);
surfc(x,y,P_rec_dBm)
title('Resived Signal Strength RSS')
xlabel('Length of Room');
ylabel('Width of Room');
zlabel('RSS in dB');
figure
contour(x,y,P_rec_dBm)
title('2D CONTUR ')
hold on
mesh(x,y,P_rec_dBm)
figure
% Calculate Noise in System
Bs = Rb*I2;
Pn = Iamp/Rb;
Ptotal = P_rec_total+Pn;
new_shot = 2*q*Ptotal*Bs;
new_amp = Iamp^2*Bn;
% Calculate SNR
new_total = new_shot + new_amp;
SNRl = (R.*P_rec_total).^2./ new_total;
```

```
SNRdb = 10*log10(SNRl);
index = index + 1;
%Plot Graph %
mesh(x,y,SNRdb);
title('SNR Distribution in Room');
xlabel('Length of Room');
ylabel('Width of Room');
zlabel('SNR in dB');
figure
C=3e8*1e-9;% time will be measured in ns in the program
rho=0.8;% reflection coefficient
m=-log10(2)/log10(cosd(theta));
Nx=lx*3; Ny=ly*3; Nz=round(lz*3);% number of grid in each surface
dA=lz*ly/(Ny*Nz);
% calculation grid area
x=-lx/2:lx/Nx:lx/2;
y=-ly/2:ly/Ny:ly/2;
z=-lz/2:lz/Nz:lz/2;
% first transmitter calculation
TP1=[0 0 lz/2];% transmitter position
TPV=[0 0 -.9];% transmitter position vector
RPV=[0 0 .9];% receiver position vector
WPV1=[.9 0 0];
WPV2=[0 .9 0];
WPV3=[-.9 0 0];
WPV4=[0 -.9 0];
% wall vectors
delta_t=1/2;% time resolution in ns, use in the form of 1/2^m
 for ii=1:Nx+1
 for jj=1:Ny+1
 RP=[x(ii) y(jj) -lz/2];
 t_vector=0:25/delta_t; % time vector in
 h_vector=zeros(1,length(t_vector));% receiver position vector
 % LOS channel gain
 D1=sqrt(dot(TP1-RP,TP1-RP));
 cosphi=lz/D1;
 tau0=D1/C;
 index=find(round(tau0/delta_t)==t_vector);
 if abs(acosd(cosphi))<=FOV

h_vector(index)=h_vector(index)+(m+1)*Adet.*cosphi.^(m+1)./(2*pi.*D1
.^ 2);
 end
 %reflection from first wall
 count=1;
 for kk=1:Ny+1
 for ll=1:Nz+1
WP1=[-lx/2 y(kk) z(ll)];
D1=sqrt(dot(TP1-WP1,TP1-WP1));
cos_phi=abs(WP1(3)-TP1(3))/D1;
cos_alpha=abs(TP1(1)-WP1(1))/D1;
D2=sqrt(dot(WP1-RP,WP1-RP));
cos_beta=abs(WP1(1)-RP(1))/D2;
cos_psi=abs(WP1(3)-RP(3))/D2;
tau1=(D1+D2)/C;
index=find(round(tau1/delta_t)==t_vector);
if abs(acosd(cos_psi))<=FOV

h_vector(index)=h_vector(index)+(m+1)*Adet*rho*dA*cos_phi^m*cos_alph
a*cos_beta*cos_psi/(2*pi^2*D1^2*D2^2);
end
```

```
 count=count+1;
 end
 end
 %% Reflection from second wall
 count=1;
 for kk=1:Nx+1
 for ll=1:Nz+1
 WP2=[x(kk) -ly/2 z(ll)];
 D1=sqrt(dot(TP1-WP2,TP1-WP2));
 cos_phi= abs(WP2(3)-TP1(3))/D1;
 cos_alpha=abs(TP1(2)-WP2(2))/D1;
 D2=sqrt(dot(WP2-RP,WP2-RP));
 cos_beta=abs(WP2(2)-RP(2))/D2;
 cos_psi=abs(WP2(3)-RP(3))/D2;
 tau2=(D1+D2)/C;
 index=find(round(tau2/delta_t)==t_vector);
 if abs(acosd(cos_psi))<=FOV

h_vector(index)=h_vector(index)+(m+1)*Adet*rho*dA*cos_phi^m*cos_alph
a*cos_beta*cos_psi/(2*pi^2*D1^2*D2^2);
 end
 count=count+1;
 end
end
 % Reflection from third wall
 count=1;
for kk=1:Ny+1
for ll=1:Nz+1
WP3=[lx/2 y(kk) z(ll)];
D1=sqrt(dot(TP1-WP3,TP1-WP3));
cos_phi= abs(WP3(3)-TP1(3))/D1;
cos_alpha=abs(TP1(1)-WP3(1))/D1;
D2=sqrt(dot(WP3-RP,WP3-RP));
cos_beta=abs(WP3(1)-RP(1))/D2;
cos_psi=abs(WP3(3)-RP(3))/D2;
tau3=(D1+D2)/C;
index=find(round(tau3/delta_t)==t_vector);
if abs(acosd(cos_psi))<=FOV

h_vector(index)=h_vector(index)+(m+1)*Adet*rho*dA*cos_phi^m*cos_alph
a*cos_beta*cos_psi/(2*pi^2*D1^2*D2^2);
end
 count=count+1;
end
end
 % Reflection from fourth wall
 count=1;
 for kk=1:Nx+1
  for ll=1:Nz+1
 WP4=[x(kk) ly/2 z(ll)];
 D1=sqrt(dot(TP1-WP4,TP1-WP4));
 cos_phi= abs(WP4(3)-TP1(3))/D1;
 cos_alpha=abs(TP1(2)-WP4(2))/D1;
 D2=sqrt(dot(WP4-RP,WP4-RP));
 cos_beta=abs(WP4(2)-RP(2))/D2;
 cos_psi=abs(WP4(3)-RP(3))/D2;
 tau4=(D1+D2)/C;
 index=find(round(tau4/delta_t)==t_vector);
    if abs(acosd(cos_psi))<=FOV
```

```
h_vector(index)=h_vector(index)+(m+1)*Adet*rho*dA*cos_phi^m*cos_alph
a*cos_beta*cos_psi/(2*pi^2*D1^2*D2^2);
    end
  count=count+1;
   end
  end
  t_vector=t_vector*delta_t;
  mean_delay(ii,jj)=sum((h_vector).^2.*t_vector)/sum(h_vector.^2);
  Drms(ii,jj)=sqrt(sum((t_vector-
mean_delay(ii,jj)).^2.*h_vector.^2)/sum(h_vector.^2));
  end
  end
  surf(x,y, Drms)
 % titel('diffuse reflection')
  xlabel('Length of Room');
  ylabel('Width of Room');
  zlabel('Drms');
```

Appendix B (outdoor VLC system model code)

```
% Description: This file is used to define all parameters.


%% simulation
Sim_Par = 'POW';  % simulation parameter; 'POW' = average optical
power is varid, 'EXR' = extention ratio is varied.
Avg_Opt_Pow_start = 0.1e-3;  % optical average power - start value
(W)
Avg_Opt_Pow_end = 5e-3;  % optical average power - stop value (W)
Avg_Opt_Pow_step = 5;  % optical average power - step value (W)
Avg_Opt_Pow_const = 100e-3;  % onstant optical average power (W)
ext_ratio_start = 2;  % extinction ratio = P_max/P_min - start value
ext_ratio_end = 200;  % extinction ratio = P_max/P_min - stop value
ext_ratio_step = 10;  % extinction ratio = P_max/P_min - step value
ext_ratio_const = 20;  % constant extinction ratio = P_max/P_min
RepOrd = 2;  % repeatation Order


%% bit operations
Sync_EN = false;  % if synchronisation is needed
NoB = 5e6;  % no of bits for each burst transmission
BR = 1e6;  % Data rate (bps)
NoS = 5;  % No of samples per bit


%% baseband modulation
lambda = 1550e-9; % laser wavelength (m)////////////
Sig_Step = 5e-3;  % signal step for each signal level (A)
BW = BR*1.25;  % bandwidth of baseband signal


%% laser
Las_Eff = 0.5;  % laser internal modulation efficiency (W/A)///////
Sig_Level = 0.5;  % a calibration constant - the DC level of optical
signal for NRZ-OOK modulation


%% background light
P_background = 0.01e-3;  % background light power (W); radiation
from diffused from sun and sky


%% geometrical loss
GL_EN = false;  % if the geometrical loss is taken into account
Prop_Mod = 'UNI';  % beam propagation/illumination model; 'UNI' =
uniform propagation/illumination, 'GUS' = Gaussian
propagation/illumination


%% lossy channel
MiscLoss = 0;  % miscellaneous channel loss (dB)
Link_Len = 500;  % link Length (m)
Fading_Add = 'M2';  % fading effect; 'M1' = fading affects average
power, 'M2' = fading affects signal, 'M3' = fading affects average
power + signal
```

```
%% fog/smoke channel
FS_EN =true;  % if the effect of fog/smoke is present
Vis_FS = 2.25;  % fog/smoke visibility (km)
lambda_0 = 1550e-9;  % reference wavelength (green light) (m)
T_th_FS = 2/100;  % contrast threshold (typical value = 2%)


%% turbulence channel
Turb_EN = false;  % if the effect of turbulence is present
Cn2 = 4e-13;  % the refractive index structure coefficient (m^-2/3)
F_t = 500;  % turbulence maximum frequency (Hz); inverse of tepmoral
coherence(1 - 10 mS)
Resamp_Turb = 'RECT';  % method of resampling the turbulence
samples; 'RES' = uses 'resample' function, 'RECT' = uses 'rectpulse'
function
Turb_Mod = 'GG';  % turbulence model; 'LN' = Log-Normal model, 'GG'
= Gamma-Gamma model


%% pointing error channel
PE_EN = false;  % if the effect of pointing errors is present
sig_j_PE = 0.5;  % pointing errors horizontal jitter (m)
mu_h_PE = 0;  % horizontal displacement
mu_v_PE = 0;  % vertical displacement
F_p = 500;  % pointing errors maximum frequency (Hz); inverse of
tepmoral coherence(1 - 10 mS)
Resamp_PE = 'RECT';  % method of resampling the pointing errors
samples; 'RES' = uses 'resample' function, 'RECT' = uses 'rectpulse'
function


%% transmitter optics
TX_AP_Type = 'ANG';  % transmitter beam parameter type; 'ANG' =
divergence angle is given, 'DIA' = Tx aperture diameter is given
Prop_Type = 'GUS';  % laser propagation model; 'GUS' = Gaussain
propagaion model, 'UNI' = uniform propagation model
theta_d_v = 10;  % full vertical divergence angle (Deg)
theta_d_h = 10;  % full horizontal divergence angle (Deg)
w_tx_v = 5e-3;  % vertical beam size (m)
w_tx_h = 5e-3;  % horizontal beam size (m)
Tx_Pos = [0; 0; 0];  % laser source cartesian position in the global
coordinate (m, m, m)
Tx_Dir = [cosd(90); sind(90); 0];  % direction of the source
propagation; cannot be 0
Tx_Ori = 0;  % orientation of the source (Deg); around local z axis


%% receiver optics
Rx_Ap_dia = 0.005;  % receiver aperture diameter (m)
Rx_Pos = [sqrt(Link_Len^2 - 2^2); 2; 0];  % receiver aperture
cartesian position in the global coordinate (m, m, m)
Rx_Dir = [cosd(45 + 180); sind(45 + 180); 0];  % direction of the
receiver aperture facing; normal to the detector face; cannot be 0
Rx_Ori = 0;  % orientation of the aperture (Deg); around local z
axis
Rx_Trn = 85;  % receiver aperture transmittance (%)
AFOV = 1;  % receiver aperture full-angle angular field-of-view
(Deg)
```

```
%% photodetector
PD_Resp = 0.5;  % responsivity of photodiode (A/W)
PD_Gain = 1e1;  % transimpedance amplifier gain (V/A)
PD_NEP = 1e-12;  % noise equivalent power (NEP) of optical receiver
(W/sqrt(Hz))
PD_RL = 50;  % receiver load impedance (Ohms)
BW_BR_r = 1.25;  % bandwidth to bit rate ratio (Hz/bps)
q_ch = 1.60217662e-19;  % electron charge (C)


%% detection
Thresh_Len_Coeff = 1;  % this coefficient is used to shorten/widen
the length of adaptive threshold estimation



%%%%%%%%%%%%%%%%%%%%%%%%%%%%%%%%%%%%%%%%%%%%%%%%%%%%%%%%%%%%%%%%%%%%%%%%
%%%%%%%
clc;  % clean the command console
clearvars;  % clean all variables in the workspace. Use 'clear all'
for older versions of MATLAB
close all;  % close all open figures, windows, etc.


%% global parameters
run('.\\GlobalParameters.m');  % load the simulation parameters


%% initialisation
run('.\\Codes\\InitialisingParameters.m');  % initialise the
simulation parameters


SNR_dB_Sim = zeros(1, Loop_Order);  % SNR array (dB)
BER_Sim = zeros(1, Loop_Order);  % BER array
Q_Sim = zeros(1, Loop_Order);  % Q-factor array
NoE_Sim = zeros(1, Loop_Order);  % no of erronous bits at each
simulation step
Threshold_Sim = zeros(NoT*Thresh_Len_Coeff + 1, Loop_Order);  %
threshold array; including values for adaptive thresholding


%% Main Loop
% calculate BER for each given parameter
for Index = 1:Loop_Order


    % ---------------------------------------------------------------
-------
    % assign the simulation parameters
    Avg_Opt_Pow = Avg_Opt_Pow_Array(Index);  % set the average
optical power
    ext_ratio = ext_ratio_Array(Index);  % set the extinction ratio

    % ---------------------------------------------------------------
-------
    % Section 2
    % laser modulation part 1
```

```
    % calculating power levels for each SNR value
    P_Sim_avg = Avg_Opt_Pow;    % calculate average optical power
    P_Sim_0 = 2*P_Sim_avg/(1 + ext_ratio);  % output power for bit 0
    P_Sim_1 = 2*P_Sim_avg/(1 + 1/ext_ratio);  % output power for bit
1
    DelP_Sim = P_Sim_1 - P_Sim_0;  % amplityde of optical signal


    % to Increase the accurary, repeat each BER step "RepOrd" times
    for Index_Rep = 1:RepOrd

        % print out information regarding current iteration
        fprintf(['Index = %d out of %d\nAverage optical power\t=
%5.3f dBm,\t %5.3f mW',...
            '\nExtinction ratio\t\t= %5.2f\n'],...
            Index, Loop_Order, 10*log10(Avg_Opt_Pow) + 30,
Avg_Opt_Pow*1e3, ext_ratio);  % print out the SNR index
        fprintf('Repetition\t\t\t\t= %d out of %d\n', Index_Rep,
RepOrd);  % print out the repetition index
        fprintf([repmat('*\t', 1, 18), '\n']);  % print out the
separater


        % ---------------------------------------------------------
-------
        % Section 1
        % Section 2
        % pseudorandom binary sequence (PRBS) generation and NRZ-OOK
bits
        Raw_Bit_Sim = randi([0, 1], 1, NoB);  % generate random bits
        Signal_Sim_Out = rectpulse(Raw_Bit_Sim, NoS);  % resample
bits


        % ---------------------------------------------------------
-------
        % Section 2
        % Section 3
        % laser modulation part 2
        % generating output optical signal based on generated OOK
signal
        % and calculated power levels
        Laser_Sim_Out = DelP_Sim*(Signal_Sim_Out - Sig_Level);  %
generate laser output (W)
        Sig_Sim_Power = var(Laser_Sim_Out);  % measure the signal
power
        clear Signal_Sim_Out;  % relesse the memory


        % ---------------------------------------------------------
-------
        % finding the 1st rising edge of signal based on transmit
signal
        % finding rising edge
        run('.\\Codes\\FindFirstRisingEdge.m');  % find the first
rising edge
```

```
        % ------------------------------------------------------------
-------
        % Section 11
        % geometrical loss effect
        if (GL_EN == true)
            run('.\\Codes\\GeometricalLoss.m');  % apply the
geometrical loss
        else
            Geo_Loss_Sim = 1;  % geometrical loss is ignored
        end


        % ------------------------------------------------------------
-------
        % Section 11
        % fog/smoke channel effect
        if (FS_EN == true)
            run('.\\Codes\\AtmosphericAttenuation.m');  % apply the
atmospheric atteaution effect
        else
            Atm_Att_Sim = 1;  % atmospheric attenuationm effet is
ignored
        end


        % ------------------------------------------------------------
-------
        % Section 9
        % Section 10
        % turbulence channel effect
        if (Turb_EN == true)
            run('.\\Codes\\TurbulenceEffect.m');  % apply the
turbulence effect
        else
            Turb_Sim = 1;  % turbulence effet is ignored
        end


        % ------------------------------------------------------------
-------
        % Section 9
        % Section 10
        % pointing error channel effect
        if (PE_EN == true)
            run('.\\Codes\\PointingErrosEffect.m');  % apply the
pointing errors effect
        else
            PE_Sim = 1;  % turbulence effet is ignored
        end


        % ------------------------------------------------------------
-------
        % Section 4
        % FSO channel effect
        Misc_Loss = 10^(-MiscLoss/10);  % total FSO channel loss
        Fading_Sim =
Misc_Loss*Geo_Loss_Sim*Atm_Att_Sim*Turb_Sim.*PE_Sim;  % channel
fading coefficient
```

```
        Mean_Fading_Sim = mean(Fading_Sim);  % mean value of the
simulated fading coefficient
        Const_Loss = Atm_Att_Sim*Geo_Loss_Sim*Misc_Loss;  % constant
loss due to atmosphere, propagation, misc loss; this loss only uses
onstant attenuation rather than varying fading
        Var_Fading_Sim = var(Fading_Sim);  % variance value of the
simulated fading coefficient
        clear Turb_Sim;  % release the memory
        clear PE_Sim;  % release the memory
        if(strcmp(Fading_Add, 'M1'))
            Rec_Sim_Opt = Fading_Sim.*P_Sim_avg + Laser_Sim_Out;  %
received optical signal after loss and turbulence effect (Method 1)
        elseif(strcmp(Fading_Add, 'M2'))
            Rec_Sim_Opt = Fading_Sim.*Laser_Sim_Out + P_Sim_avg;  %
received optical signal after loss and turbulence effect (Method 2)
        elseif(strcmp(Fading_Add, 'M3'))
            Rec_Sim_Opt = Fading_Sim.*(Laser_Sim_Out + P_Sim_avg);
% received optical signal after loss and turbulence effect (Method
3)
        else
            error('pick a fading implementation method');  % print
out an error message and exit
        end
        fprintf('Channel Coefficient:\tMean Value\t\t= %.3f\n',...
            Mean_Fading_Sim);  % print out the mean value
        fprintf('Channel Coefficient:\tVar Value\t\t= %.3f\n',...
            Var_Fading_Sim);  % print out the mean value
        fprintf('Channel Coefficient:\tConstant Loss\t= %.3f
dB\n',...
            -10*log10(Const_Loss));  % print out the mean value
        clear Laser_Sim_Out  % release the memory
        clear Fading_Sim;  % release the memory


        % ---------------------------------------------------------
-------
        % Section 5
        % optical to electical coversion (photodetector)
        Rec_Sim_Sig = PD_Resp*PD_Gain*Rec_Sim_Opt;  % PD conversion
        clear Rec_Sim_Opt;  % release the memory


        % ---------------------------------------------------------
-------
        % Section 6
        % applying SNR to the received signal
        P_noise_SHN =
(PD_Gain^2)*(2*q_ch*PD_Resp*Avg_Opt_Pow*Const_Loss*BW)/PD_RL;  %
total power of noise (W) due to shot noise
        P_noise = P_noise_NEP + P_noise_SHN + P_noise_BGD;  % total
power of noise (W)
        Rec_Sim_Sig_Power =
((Const_Loss*PD_Resp*PD_Gain)^2*Sig_Sim_Power)/PD_RL;  % received
signal power (W); normalised to 50 Ohms
        SNR = Rec_Sim_Sig_Power/P_noise;  % signal-to-noise ratio
(SNR)
        SNR_dB_Sim(Index) = 10*log10(SNR);  % update SNR array with
SNR (dB)
        AdditiveNoise_Sim = randn(1, NoP)*sqrt(P_noise*PD_RL);  %
generating white Gaussian noise
```

```
        Det_Sim_Sig = Rec_Sim_Sig + AdditiveNoise_Sim;  % adding
white Gaussian noise to the detected signal
        clear Rec_Sim_Sig;  % release the memory
        clear AdditiveNoise_Sim;  % release the memory


        % ---------------------------------------------------------
-------
        % performing signall processing on detected electical signal
        LPF_RX_Sim_1 = Det_Sim_Sig - mean(Det_Sim_Sig);  % remove DC
level
        P2P_RX_Sim = std(LPF_RX_Sim_1)*2;  % calculate peak-to-peak
of received signal
        LPF_RX_Sim_2 = LPF_RX_Sim_1/P2P_RX_Sim;  % normalise
received signal
        clear Det_Sim_Sig;  % release the memory
        RX_Sim_OOK = LPF_RX_Sim_2((Index_RE +
round(NoS/2)):NoS:end);  % sample and hold the detected signal
        clear LPF_RX_Sim_1;  % release the memory
        clear LPF_RX_Sim_2;  % release the memory


        % ---------------------------------------------------------
-------
        % Section 8
        % analysing detected signal
        % calculating Q-factor parameters
        SigLength = length(RX_Sim_OOK);  % sampled signal length
        run('.\\Codes\\QFactorExtractor.m');  % calculate Q-factor


        % ---------------------------------------------------------
-------
        % Section 7
        % thresholding and extract the bits
        % generating transmit bits matrix
        run('.\\Codes\\Quantisation.m');  % extract bits from the
received signal


        % ---------------------------------------------------------
-------
        % Section 8
        % BER calculation
        [NoE_Sim_Temp, BER_Sim_Temp] = biterr(TX_OOK_bit,
RX_Sim_OOK_bit);  % calculate BER and no of erronous bits
        clear TX_OOK_bit;  % release the memory
        clear RX_Sim_OOK_bit;  % release the memory
        BER_Sim(Index) = BER_Sim(Index) + BER_Sim_Temp;  % update
the BER array for each iteration
        NoE_Sim(Index) = NoE_Sim(Index) + NoE_Sim_Temp;  % update
the no of errors array for each iteration
        Q_Sim(Index) = Q_Sim(Index) + Q_Fac;  % update the Q factor
array for each iteration


        % ---------------------------------------------------------
-------
        % signal detection presentaion for each iteration
```

```
        fprintf(['SNR\t\t\t= %4.2f dB,\tBER\t\t\t= %5.3g\n',....
            'Threshold\t= %5.3f,\tQ-factor\t= %5.3f\n\n'],...
            SNR_dB_Sim(Index), BER_Sim_Temp, Threshold_Sim_Temp,
Q_Fac);  % print out the received signal properties for each
iteration

    end

    % ------------------------------------------------------------------
---
    % BER calculation for each SNR
    BER_Sim(Index) = BER_Sim(Index)/RepOrd;  % update the BER array
    Threshold_Sim(Index) = Threshold_Sim(Index)/RepOrd;  % update
the threshold array
    Q_Sim(Index) = Q_Sim(Index)/RepOrd;  % update the Q-factor array

    % ------------------------------------------------------------------
---
    % signal detection presentaion for each SNR
    fprintf('SNR\t\t\t\t= %4.2f\nAverage BER\t\t= %5.3g\nAverage
Threshold\t= %5.3f\nAverage Q-factor\t= %5.3f\n',...
        SNR_dB_Sim(Index), BER_Sim(Index), Threshold_Sim(1, Index),
Q_Sim(Index));  % print out the received signal properties for each
SNR
    fprintf([repmat('-', 1, 70), '\n']);  % print out the separater

end


%% analytical initialisation
eta = 1;  % responsivity for theoritical BER
N0 = 1;  % noise spectral density for theoritical BER
k_ord_GH = 400;  % no of Gaussï¿½Hermite quadrature series expansion
for theoritical BER
k_ord_GL = 50;  % no of Gaussï¿½Laguerre quadrature series expansion
for theoritical BER
SNR_dB_Anl = linspace(SNR_dB_Sim(1), SNR_dB_Sim(end), 100);  % SNR
(dB) array for theoritical BER
SNR_Anl = 10.^(SNR_dB_Anl/10);  % SNR array for theoritical BER
I0 = sqrt(N0*2*SNR_Anl)/eta;  % intensity for theoritical BER


%% theoritical BER calculation
% theoritical analysis - pointing errors
run('.\\Codes\\PointingErrorsBER.m');  % calculating analytical BER
based on Log-Normal model

% theoritical analysis - weak turbulence
run('.\\Codes\\LogNormalBER.m');  % calculating analytical BER based
on Log-Normal model

% theoritical analysis - strong turbulence
run('.\\Codes\\GammaGammaBER.m');  % calculating analytical BER
based on Gamma-Gamma model

% theoritical analysis - pointing errors + weak turbulence
run('.\\Codes\\PointingErrorsLogNormalBER.m');  % calculating
analytical BER based on Gamma-Gamma model
```

```
% theoritical analysis - pointing errors + strong turbulence
run('.\\Codes\\PointingErrorsGammaGammaBER.m');  % calculating
analytical BER based on Gamma-Gamma model

% theoritical analysis - clear channel
run('.\\Codes\\ClearChannelBER.m');  % calculating analytical BER
over clear channel

% theoritical analysis - fog/smoke channel
run('.\\Codes\\FSChannelBER.m');  % calculating analytical BER over
clear channel


%% plotting Results
Style = {'', 'o', '*', 's', '^', 'h', 'x', '+', 'd', 'v', '<', '>',
'p'};

figure;  % create and empty figure window
hold on;  % hold all plots
box on;  % make the box around the axis visible
Sim_Type = '';  % simulation type; used for changing the name of the
output graph

% generate the proper plot title for each simulation scenario
if((Turb_EN == false) && (PE_EN == false) && (FS_EN == false))  %
clear channel case
    MarkerPlot(SNR_dB_Anl, BER_Anl_cl, 'b', '-', Style{1}, 10);
    str_par = 'clear channel';
    Sim_Type = '-Clear_Channel';  % adjust simulation type variable
elseif((Turb_EN == false) && (PE_EN == false) && (FS_EN == true))  %
fog/smoke channel case
    MarkerPlot(SNR_dB_Anl, BER_Anl_fs, 'b', '-', Style{1}, 10);
    str_par = 'fog/smoke channel';
    Sim_Type = '-Fog_Channel';  % adjust simulation type variable
elseif((Turb_EN == false) && (PE_EN == true))  % pointing errors
channel case
    MarkerPlot(SNR_dB_Anl, BER_Anl_PE, 'b', '-', Style{1}, 10);
    str_par = sprintf('pointing error channel with \\sigma_{j} =
%4.2f', sig_j_PE);
    Sim_Type = '-PE_Channel';  % adjust simulation type variable
elseif((Turb_EN == true) && (PE_EN == false) && strcmp(Turb_Mod,
'LN'))  % log-normal turbulence channel case
    MarkerPlot(SNR_dB_Anl, BER_Anl_LN_turb, 'b', '-', Style{1}, 10);
    str_par = sprintf('turbulence channel (Log-Normal model) with
\\sigma_{R}^2 = %4.2f', sig2_R_Sim);
    Sim_Type = '-LN_Channel';  % adjust simulation type variable
elseif((Turb_EN == true) && (PE_EN == false) && strcmp(Turb_Mod,
'GG'))  % gamma-gamma turbulence channel case
    MarkerPlot(SNR_dB_Anl, BER_Anl_GG_turb, 'b', '-', Style{1}, 10);
    str_par = sprintf('turbulence channel (Gamma-Gamma model) with
\\sigma_{R}^2 = %4.2f', sig2_R_Sim);
    Sim_Type = '-GG_Channel';  % adjust simulation type variable
elseif((Turb_EN == true) && (PE_EN == true) && strcmp(Turb_Mod,
'LN'))  % log-normal turbulence + pointing errors channel case
    MarkerPlot(SNR_dB_Anl, BER_Anl_PE_LN_turb, 'b', '-', Style{1},
10);
    str_par = sprintf(['turbulence channel (Log-Normal model) with
\\sigma_{R}^2 = %4.2f\n'...
        'and pointing error channel with \\sigma_{j} = %4.2f'],
sig2_R_Sim, sig_j_PE);
```

```
    Sim_Type = '-LN_PE_Channel';  % adjust simulation type variable
elseif((Turb_EN == true) && (PE_EN == true) && strcmp(Turb_Mod,
'GG'))  % gamma-gamma turbulence + pointing errors channel case
    MarkerPlot(SNR_dB_Anl, BER_Anl_PE_GG_turb, 'b', '-', Style{1},
10);
    str_par = sprintf(['turbulence channel (Gamma-Gamma model) with
\\sigma_{R}^2 = %4.2f\n'...
        'and pointing error channel with \\sigma_{j} = %4.2f'],
sig2_R_Sim, sig_j_PE);
    Sim_Type = '-GG_PE_Channel';  % adjust simulation type variable
end

MarkerPlot(SNR_dB_Sim, BER_Sim, 'r', '--', Style{2}, 10);  % plot
BER vs. SNR curve
Dummy = BER_Sim(BER_Sim > 0);  % isolate non-zero BER values
axis([SNR_dB_Sim(1), SNR_dB_Sim(end), min(Dummy), 1]);  % auto
adjust the plot axis
xlabel('SNR (dB)');  % label x axis
ylabel('BER');  % label y axis

str_title = sprintf('BER vs. SNR for %s', str_par);  % forma the
title text
title(str_title);  % create the title

MakeitPretty(gcf, [10, 9], ['L', 'G'], [12, 1.5, 5, 10],
['.\\Graphs\\BER_SNR', Sim_Type]);  % format the plot
```

PDF-XChange Editor
Click to BUY NOW!
www.tracker-software.com

PDF-XChange Editor
Click to BUY NOW!
www.tracker-software.com

PDF-XChange Editor
Click to BUY NOW!
www.tracker-software.com

PDF-XChange Editor
Click to BUY NOW!
www.tracker-software.com

PDF-XChange Editor
Click to BUY NOW!
www.tracker-software.com